



D E P A R T M E N T O F
GEOGRAPHICAL SCIENCES
AT THE UNIVERSITY OF MARYLAND, COLLEGE PARK

26 November, 2015

Dear Dr. Bahn,

Thank you for overseeing the review of our manuscript, *Characterizing Leaf Area Index (LAI) and Vertical Foliage Profile (VFP) over the United States*. We are pleased to provide a revision of our paper. We thank the reviewers for their careful comments and have responded to all concerns with suitable modifications to the manuscript. The manuscript has certainly improved following these feedbacks from the reviewers.

In specific, we added all relevant equations deriving LAI and its vertical profiles from ICESat data in the supplement for easy reference. We included statistical results into figures whenever necessary. We also fixed minor problems related to typo or unclear variable definition.

We hope you will now found our paper suitable for publication.

Sincerely,

Hao Tang

University of Maryland

College Park, MD

We thank the two referees for their insight and very helpful comments. Below are our detailed responses to their concerns respectively:

Referee #1

General Comments:

A) Section 2.2. Leaf-off season is indeed from November to March, but for maximum foliage, it would be recommended to use May to September shots only. Can you provide a short evaluation of shots chosen in leaf flushing and senescence periods? This factor may be responsible for your negative LAI bias.

The referee is correct about the bias introduced by seasonality, and a simple average of GLAS LAI over different months supports this hypothesis: 3.02 for May, 3.14 for June, 2.93 for October and 2.22 for November.

However, we did not exclude the leaf flushing/senescence periods because we tried to maximize the usage of GLAS shots. The GLAS/ICESat mission was not operated year round but deployed for three 33-day campaigns per year due to defects in laser design which required it to maximize its operations for ice sheets (Schutz et al., 2005). The starting dates of each campaign were around mid-February, mid-May and early-October. The sampling bias caused by not using the October data, given how few shots we would have otherwise, far outweighed the small potential bias of using these data for continental scale mapping.

B) Section 2.2. An equation defining the gap profile derived from the lidar waveform, and/or the choice of variables, e.g. the clumping factor if used and the g function. Just a little more information about this would be useful.

We thank the referee for this helpful comment. We have now included all relevant equations in the supplement for easy reference, while also referring readers to the original equations and variables in Tang et al. 2014a and 2014b.

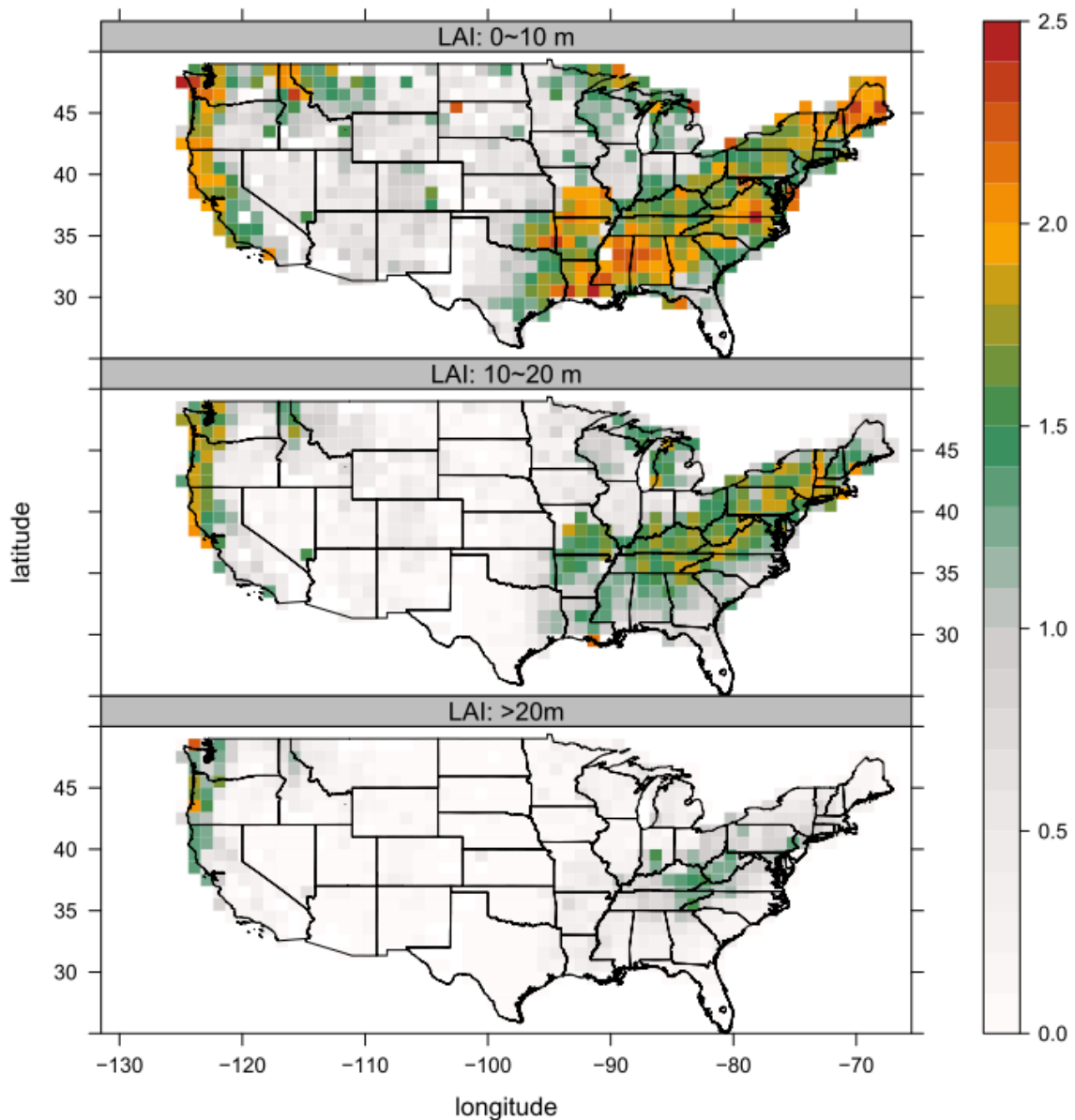
C) Section 3.2 paragraph 2. Figure 3 and Figure 6 should be in sync. Do not present 5 m intervals if your final qualitative product is in 10m intervals. Either also present the 10 m intervals or only present 10m.

We understand this point and debated whether to show them at the same intervals before submission. We decided it was more informative to show different intervals for the following reasons. Figure 3 shows that the accuracy of vertical foliage profile (VFP) varies at different height layers with lowest value in the understory (0 - 5 m). This result is very important because there is a large uncertainty of GLAS VFP at fine vertical resolutions (5 m or smaller) and therefore the product may not be reliable close to the ground. Secondly, the comparisons between Figure 1 and Figure 3 suggest that the accuracy of VFP is also dependent on the length of the integration interval, and a longer interval will lead to a higher accuracy (see Discussion P13686L26 - P13687L5). So the take home message is that the product is better used at 10 m intervals vs. 5 m, but this is really only evident if we actually show the 5 m intervals. When we then produce the continental map we naturally want the

maps to be as accurate as possible a depiction of reality, and this is best achieved by going to 10 m intervals. So the two figures are serving different purposes and we still feel that it is probably better to keep them as they are.

D) I agree that showing the LAI for the WWF regions is significant, and an important result. What would also be useful would be to present LAIs for large gridded areas over the contiguous US, e.g. 1-3 degrees depending on the density of the GLAS pulses. This may also tie in well with the comparisons to elevation, forest cover, and precipitation. In fact, these could be presented alongside.

Thank you for the suggestion. We have calculated 1 degree maps and now present these in the Supplement (shown below).



Specific Comments

1) P. 13681 Lin 10. 3x3 what?

3×3 Landsat window

2) Figure 2 & 3. Put the RMSE and R2 and bias on these figures or on the caption.

Thank you. All three have been put on the figures.

3) Figure 2 caption: 'Each VFP point represents an integrated value of foliage density at 5m height interval.' Change this to '. . . at each 5m height interval' or '. . .for all 5m height intervals'.

Thank you. We have changed this to '. . . at each 5m height interval'

4) Figure 9&10. Not sure why the boxplots are of different sizes. This is cosmetic, but some would prefer the same sizes.

The standard visualization for data distributions using box plots is that their length corresponds the quartile values, the whiskers give the extremes of the range, and the widths are proportional to the actual number of observations. We would prefer to keep this standard.

5) Section 3.3: By Forest Ratios do you mean canopy cover defined by some passive satellite? This is not clear. Do you use land class products under the footprint to define forested pixels vs non forested?

Thank you for pointing this out. The Forest Ratio uses a MODIS land cover map to derive the number of GLAS shots that are classified as being over forest or non-forest (and the ratio gives this percentage). We have added a reference to its definition in Section 3.3 and Figure 9 (p13684 line 22): Each GLAS footprint was classified as either forest or non-forest with an overlay of MODIS land cover map, and the Forest Ratio was defined as the percentage of footprints classified as forests in total GLAS shots within each elevation group..

6) Are all your boxplots in Fig 9 & 10 equivalent to your ecoregions, or some predefined grid size?

The boxplots are not related to ecoregion. In each plot, the boxes represent a range of the value being associated with LAI (precipitation or elevation) to illustrate the relationship of LAI to these variables. The relationships are much easier to see when binned into classes.

7) P. 13686 line2. Pedantic. . .but perhaps don't use 'reasonable'.

Thank you. We changed the word 'reasonable' to 'acceptable'

8) P. 13687. Are GLAS LAIs derived from the raw waveform or the modelled 6 Gaussians?

GLAS LAI were derived from the raw waveform. The modeled Gaussians were internal variables used in the algorithm. More details can be found in Tang et al. 2014a.

Referee #2

GENERAL COMMENTS

My main concern is about the presentation of the GLAS LAI over US (Figure 5). This figure does not help much about our understanding of the LAI distribution but may even lead to misunderstandings, because of the overly simple statistics at the ecoregion level. I would suggest the authors to draw dotted maps or gridded maps in 65 m resolution, that may give readers a better concept of the GLAS LAI. Grassland and crop types may be avoided, as they are not discussed in the text and may have been severely underestimated. Likewise, I doubt the value of the LAI statistics in Table 1. The standard deviations are rather high, many times larger than the mean LAI values, because of the huge diversity over an ecoregion.

While we understand the reviewer's concern about mapping at the ecoregion level, it is impossible to map at the suggested scale because ICESAT is a transecting mission. It does not provide wall-to-wall coverage, but rather only provides along track samples spaced about 100 m apart but with cross-track distances as large as 30 km. Therefore, the only way to provide a continuous map of LAI intervals is by mapping the samples into *strata*. In our case, we chose ecoregions as those strata for reasons explained in our response to reviewer #1. Once this concept is understood (that we have samples and are mapping into strata), there should be no misunderstanding as to what the maps represent. We stress furthermore that these are the first maps to show the vertical distribution of LAI, not just total LAI, on a continental basis and thus represent a substantive contribution.

In terms of the variability of LAI given in Table 1, the statistics are correct. Again, the mapping into strata explains why the standard deviations are large, but they are certainly not "many times larger than the mean LAI values" as the referee asserts. Table 1 gives 40 pairs of mean-s.d. values (10 ecoregions * 1 Total LAI * 3 LAI layers). None of the total LAI values (column 1 in Table 1) have a s.d. that exceeds the mean, and indeed the C.V. is about 50% which is quite reasonable. For the layer values, the mean and s.d. are at about the same magnitude with the s.d. being larger for the highest layer. This latter point is understandable given that canopy shape and canopy top height variability will be a large driver of LAI variability in the top-most layer. Thus, the statistics given in Table 1 are consistent with the physical and sampling processes and provide considerable insight into the maps.

A fine validation of the GLAS LAI over the conterminous US may only be realized through comparison with existing Landsat and MODIS LAI. My understanding is that the Landsat LAI was generated over California only (Ganguly et al. 2012). Please provide the proper reference for the Landsat LAI over the US, which was used in the comparison with the GLAS LAI (Figure 4). I would like to know the quality of the

Landsat LAI maps over US. I strongly encourage the authors to further compare GLAS LAI with MODIS LAI, as was done in their earlier study (Tang et al. 2014). This won't be much effort based on what has been done by the authors. Moreover, please note the differences between the Landsat and MODIS estimated LAIs and the lidar derived Plant Area Index (PAI), even though they may be numerically similar (Tang et al. 2014).

Validation of GLAS LAI: We have presented a coherent series of papers that has addressed the issue of validation in the Tang et al. publications that go from physical theory to ground-based validations to airborne lidar validations that are then linked to GLAS, to Landsat and to MODIS. Our experience is that the scale of MODIS is too coarse to serve as a validation for GLAS, and there are generally too few ICESAT samples within a MODIS pixel to make this comparison very illuminating (and Tang et al, 2014a show that the data sets have low correlation). In contrast, Landsat is much more appropriate because the spatial scales match, but as we have shown in the earlier Tang et al. work and again here, Landsat LAI saturates, not just against ICESAT, but against airborne lidar data. Therefore, really the question should be turned on its head: it is the GLAS data that can be used to validate the Landsat data, again given the progression of research we have presented over the three papers.

Landsat LAI Validation: We have added a reference for the U.S. Landsat LAI product as "In Prep". While the data set is finished it is not yet published. The accuracy of the Landsat data set is in part given by the results we show here in our comparison of GLAS LAI to Landsat. It is again obvious that Landsat saturates, as has been shown in our previous research.

LAI vs. PAI: We would like to argue that the LAI derived from Landsat or MODIS is actually plant area index (PAI) too, because non-foilage elements can contribute to their reflected radiometric signal (Garrigues et al. 2008) in a similar mechanism to that of the lidar sensor. Because the lidar observation is in the near-IR, it is not nearly as sensitive to branches as leaves. Nevertheless, its contribution is generally of secondary importance, and we have discussed this issue in Tang et al. (2014a).

I'm not in favor of the environmental studies in Section 3.3. It would be more interesting to look into the seasonal LAI and VFP variations since the multi-year data are available.

The GLAS/ICESat mission was not operated across full year round but deployed for three 33-day campaigns per year due to deficits in laser design (Schutz et al., 2005). The starting dates of each campaign were around mid-February, mid-May and early-October, and the ground tracks did not repeat each year. As a result, it is impossible to do an effective seasonal study. The environmental analyses per se showed interesting results, and therefore we favor their inclusion.

DETAILED COMMENTS

contiguous United States -> conterminous United States. The latter is more used in authoritative publications.

Both terms mean the same thing (the lower 48 states) and each are widely used. We have added a definition of CONUS to clarify the ambiguity in P13676L6.

P13677L24. Saturation is also an issue for lidar LAI estimations. Likewise, I disagree with the statement in P13687L17 "the non-saturation advantage of lidar data against passive remote sensing in observing high LAI forests".

Our comparison results between airborne LVIS and destructively-sampled field data in the La Selva Biological Station have demonstrated that lidar-derived LAI did not saturate even when the LAI exceeding $10 \text{ m}^2/\text{m}^2$. We are also testing our results over other dense forests and do not see any saturation trend towards high LAI yet. Under the vast majority of real forests, it is highly unlikely that lidar will saturate, provided there is enough laser energy to get a return signal from the ground, but this is an entirely different issue. We are not clear why the referee disagrees with the statement. Everywhere we have looked, Landsat saturates and lidar does not. For this paper, all we can do is reference our previous work, and provide the results of the experiment presented. Our conclusions for the work presented in this paper are well-supported by the results.

P13679L3. Full name for CONUS

The full name has been added.

Section 2.2. P13680L4-9. Please briefly introduce the methods here, rather than referring to other papers.

We thank the referee for this helpful comment. We have added a supplement to describe necessary details of the methods, since our primary focus here is the large-scale comparison and validation of GLAS LAI and VFP data set.

Section 2.3 How good are the LVIS retrievals compared to field measurements? Please mark the four LVIS field sites in Fig. 5. Please put all resultant R2, bias, and RMSE in the figures. Only introduce them in the text when necessary.

LVIS LAI have shown excellent agreement with field measurements from destructively sampled data, hemispherical photos, LAI-2000 and terrestrial scanning lidar across different landscapes (Tang et al., 2012 and 2014a; Zhao et al., 2011 and 2012). The r^2 varies from 0.63 to 0.85, and the error varies from 0.52 to 1.36.

All four LVIS sites have been marked in Figure 5 now.

We have added those statistical results in Figures 1 - 4 while we prefer to also repeat these within the text.

P13685L7-10. The Pearsno's correlation was not shown. Why this is relevant anyway?

All Pearson's correlation coefficients are listed in the text specified. The analyses are relevant towards developing an understanding of how LAI may be correlated with environmental variables and how strong these are.

P13686L11. Slope may be a factor. How's the topography of the four validation sites?

Slope is indeed a very important factor on the derived LAI and VFP product as we have discussed in this paper and previous publications (Tang et al. 2014a and 2014b). Only Sierra Nevada forests have very rugged topography with slopes exceeding 30°, and our previous work suggests that best agreement can only be achieved with slopes less than 20°.

P13687L18-19. Fig. 4a shows that GLAS underestimates for all LAI values. Please discuss.

We discussed this in P13687L15-26, and we think there are multiple factors contributing to this relative underestimation, including differences in land cover classification schemes, adjustment of clumping effect, and data acquisition strategy.

Garrigues, S., Lacaze, R., Baret, F., Morisette, J.T., Weiss, M., Nickeson, J.E., Fernandes, R., Plummer, S., Shabanov, N.V., Myneni, R.B., Knyazikhin, Y., & Yang, W. (2008). Validation and intercomparison of global Leaf Area Index products derived from remote sensing data. *Journal of Geophysical Research-Biogeosciences*, 113, -

Schutz, B.E., Zwally, H.J., Shuman, C.A., Hancock, D., & DiMarzio, J.P. (2005). Overview of the ICESat Mission. *Geophysical Research Letters*, 32

Tang, H., Brolly, M., Zhao, F., Strahler, A.H., Schaaf, C.L., Ganguly, S., Zhang, G., & Dubayah, R. (2014a). Deriving and validating Leaf Area Index (LAI) at multiple spatial scales through lidar remote sensing: A case study in Sierra National Forest, CA. *Remote Sensing of Environment*, 143, 131-141

Tang, H., Dubayah, R., Brolly, M., Ganguly, S., & Zhang, G. (2014b). Large-scale retrieval of leaf area index and vertical foliage profile from the spaceborne waveform lidar (GLAS/ICESat). *Remote Sensing of Environment*, 154, 8-18

Tang, H., Dubayah, R., Swatantran, A., Hofton, M., Sheldon, S., Clark, D.B., & Blair, B. (2012). Retrieval of vertical LAI profiles over tropical rain forests using waveform lidar at La Selva, Costa Rica. *Remote Sensing of Environment*, 124, 242-250

Zhao, F., Strahler, A.H., Schaaf, C.L., Yao, T., Yang, X., Wang, Z., Schull, M.A., Román, M.O., Woodcock, C.E., Olofsson, P., Ni-Meister, W., Jupp, D.L.B., Lovell, J.L., Culvenor, D.S., & Newnham, G.J. (2012). Measuring gap fraction, element clumping index and LAI in Sierra Forest stands using a full-waveform ground-based lidar. *Remote Sensing of Environment*, 125, 73-79

Zhao, F., Yang, X.Y., Schull, M.A., Roman-Colon, M.O., Yao, T., Wang, Z.S., Zhang, Q.L., Jupp, D.L.B., Lovell, J.L., Culvenor, D.S., Newnham, G.J., Richardson, A.D., Ni-Meister,

W., Schaaf, C.L., Woodcock, C.E., & Strahler, A.H. (2011). Measuring effective leaf area index, foliage profile, and stand height in New England forest stands using a full-waveform ground-based lidar. *Remote Sensing of Environment*, 115, 2954-2964

1 Characterizing Leaf Area Index (LAI) and Vertical Foliage 2 Profile (VFP) over the United States

3
4 H. Tang¹, S. Ganguly², G. Zhang², M. A. Hofton¹, R. F. Nelson³, and R. Dubayah¹

5 [1] {Department of Geographical Sciences, University of Maryland, College Park, Maryland,
6 USA}

7 [2] {Bay Area Environmental Research Institute (BAERI) / NASA Ames Research Center,
8 Moffett Field, California, USA}

9 [3] {Biospheric Sciences Branch, Code 618, NASA Goddard Space Flight Center, Greenbelt,
10 Maryland, USA}

11 Correspondence to: H. Tang (htang@umd.edu)

12 13 Abstract

14 Leaf area index (LAI) and vertical foliage profile (VFP) are among the important canopy
15 structural variables. Recent advances in lidar remote sensing technology have demonstrated the
16 capability of accurately mapping LAI and VFP over large areas. The primary objective of this
17 study was to derive and validate a LAI and VFP product over the contiguous United States
18 (CONUS) using spaceborne waveform lidar data. This product was derived at the footprint level
19 from the Geoscience Laser Altimeter System (GLAS) using a biophysical model. We validated
20 GLAS derived LAI and VFP across major forest biomes using airborne waveform lidar. The
21 comparison results showed that GLAS retrievals of total LAI were generally accurate with little
22 bias ($r^2 = 0.67$, bias = -0.13, RMSE = 0.75). The derivations of GLAS retrievals of VFP within
23 layers was not as accurate overall ($r^2 = 0.36$, bias = -0.04, RMSE = 0.26), and these varied as a
24 function of height, increasing from understory to overstory - 0 to 5 m layer: $r^2 = 0.04$, bias =
25 0.09, RMSE = 0.31; 10 to 15 m layer: $r^2 = 0.53$, bias = -0.08, RMSE = 0.22; and 15 to 20 m layer:
26 $r^2 = 0.66$, bias = -0.05, RMSE = 0.20. Significant relationships were also found between GLAS

1 LAI products and different environmental factors, in particular elevation and annual precipitation.
2 In summary, our results provide a unique insight into vertical canopy structure distribution across
3 North American ecosystems. This data set is a first step towards a baseline of canopy structure
4 needed for evaluating climate and land use induced forest changes at continental scale in the
5 future and should help deepen our understanding of the role of vertical canopy structure on
6 terrestrial ecosystem processes across varying scales.

7

8 **1 Introduction**

9 Accurate measurements of three dimensional canopy structure and function play a key role in
10 global carbon dynamics, climate feedbacks as well as biodiversity studies (Heimann and
11 Reichstein, 2008;Loreau et al., 2001;Cramer et al., 2001;Schimel et al., 2001). Spatial variations
12 of ecosystem structure largely inform the geographical patterns of ecological processes, including
13 species richness (Cramer et al., 2001;Goetz et al., 2007;Turner et al., 2003). These structural
14 variables, such as canopy height, leaf area index (LAI) and vertical foliage profile (VFP), have
15 been identified as essential climate variables (ECV), essential biodiversity variables (EBV) or
16 both (Pereira et al., 2013;Aber, 1979;Gower and Norman, 1991;Baret et al., 2013). Yet
17 measurements of these canopy structural data are often limited at field sites, and their spatial
18 distributions over broader geographical areas still remain poorly characterized due to
19 heterogeneity of natural vegetation and inexact measuring techniques (Clark and Kellner,
20 2012;Asner et al., 2013). Improved spatial characterization of LAI and VFP at large scales may
21 fill this observational gap and help clarify the role of spatial and vertical variability in canopy
22 structure for carbon cycling, biodiversity and habitat quality (Houghton, 2007;Sauer et al., 2008).

23 Several global scale LAI products have been created from passive remote sensing data for many
24 years (Myneni et al., 2002;Ganguly et al., 2012;Deng et al., 2006;Baret et al., 2007). Most of
25 these products are derived by exploring the correlation between canopy foliage density and the
26 total reflected intensity of electromagnetic radiation at multiple wavelengths. Applications of
27 these LAI products have significantly improved the representation of the dynamics of terrestrial
28 ecosystems and their interactions with the atmosphere (Mu et al., 2007;Zhao et al.,
29 2005;Randerson et al., 2009). However, the overall accuracy of these products does not meet the

1 requirements as specified by Global Terrestrial Observing System (GTOS:
2 <http://www.fao.org/gtos/org.html>), and a key problem is the saturation of spectral signal over
3 dense forests with high canopy cover (Abuelgasim et al., 2006;Shabanov et al., 2005;Yang et al.,
4 2006). Saturation occurs because the solar flux decreases exponentially as it passes through a
5 dense canopy, and the majority of the returned signal comes from the upper canopy in the form of
6 direct reflectance and multiple scattering (Gower and Norman, 1991;Nilson, 1971). This limits
7 the observational capabilities of passive optical sensors, such as Landsat and MODIS, to estimate
8 LAI over dense forests. Furthermore, deriving the foliage profile as a function of height is beyond
9 the capability of passive optical remote sensing unless multiple look angles are used (Chopping et
10 al., 2009). We argue that spaceborne lidar (light detection and ranging) technology provides a
11 means of overcoming this limitation and of measuring vertical structure even over dense forests.

12 Lidar has proven effective at measuring three dimensional canopy structural information (Lefsky
13 et al., 2002). Lidar measures the distance between a target and the sensor by the round-trip
14 traveling time of an emitted laser pulse. It allows direct 3D measurements of canopy structural
15 components, including foliage, branch and trunk which then be used to estimate biophysical
16 variables, such as canopy height and biomass (Drake et al., 2002;Saatchi et al., 2011;Los et al.,
17 2012;Lefsky, 2010;Simard et al., 2011;Asner et al., 2012;Baccini et al., 2012;Strahler et al.,
18 2008), as well as LAI and VFP (Morsdorf et al., 2006;Tang et al., 2012;Zhao et al., 2013).

19 Garcia et al. (2012) and Luo et al. (2013) demonstrated the possibility of deriving LAI and VFP
20 data across different landscapes from Geoscience Laser Altimeter System (GLAS) on board of
21 Ice, Cloud and land Elevation Satellite (ICESat). Tang et al. (2014a) derived LAI and VFP data
22 from GLAS data, but using a physically based model rather than an empirical methodology. The
23 use of a physical model greatly simplified application over large areas because site specific,
24 statistical calibrations were not required. Further improvement of the model led to a GLAS LAI
25 and VFP product over the entire state of California, USA (Tang et al., 2014b). However, there is
26 still a need to further examine the relationship between vertical foliage distribution and lidar
27 waveforms over even broader areas. Assessment of their relationship across different forest types
28 and environmental gradients will not only strengthen our confidence in acquiring a potential
29 global LAI and VFP measurement, but will also provide guidance on the design and science

1 definition of future lidar missions such as the Global Ecosystem Dynamics Investigation (GEDI)
2 (Dubayah et al., 2014).

3 The objective of this study is to characterize the continental scale variability of canopy structure
4 across the United States using lidar observations from space. First, we implement our existing
5 algorithm at the GLAS footprint level and compare the derived data with LAI and VFP products
6 from airborne lidar in different forest types. Next we map the aggregated LAI and VFP product
7 according to different ecoregions and land cover types over [the Contiguous United States](#)
8 [\(CONUS\)](#). Finally we analyze the distribution of GLAS LAI across different environmental
9 factors, including elevation and precipitation.

10

11 **2 Methods**

12 **2.1 GLAS Data**

13 GLAS is a spaceborne, sampling waveform lidar sensor with the working wavelength in the near-
14 infrared band (1064 nm). It emits laser pulses at a frequency of 40 Hz and records the energy
15 reflected from both the ground surface and canopy in an approximately 65 m diameter footprint
16 (Abshire et al., 2005). GLAS samples the Earth surface in transects with individual footprints
17 separated by ~ 175 m along track, and with between track spacing that varies as a function of
18 latitude (e.g. 30 km spacing between tracks at the equator and 5 km spacing at 80° latitude
19 (Brenner et al., 2012)). As a result of this sampling pattern, GLAS does not provide a wall-to-
20 wall observation of forests. Its spatial allocation of laser footprints is best defined as a pseudo-
21 systematic sampling or cluster sampling strategy (Stahl et al., 2011;Healey et al., 2012). To
22 obtain a spatially continuous estimate of LAI at continental scale, footprint level GLAS data
23 would need to be extrapolated using other remote sensing data (Dubayah et al., 2008;Lefsky,
24 2010), or can be mapped into appropriate geographic strata such as land cover types or
25 ecoregions.

1 **2.2 Retrieval of GLAS LAI and VFP**

2 We collected a total of 1,100,498 cloud-free GLAS data from Campaigns GLA01 and GLA14
3 data over the contiguous United States from 2003 to 2007. GLA01 included the complete
4 recorded waveform at a vertical resolution of 15 cm for land surface products, and GLA14
5 products were comprised of geographical information and various parameters calculated from the
6 waveform (Harding and Carabajal, 2005). Low energy shots (peak energy < 0.5 Volt) were
7 excluded from data process for retrieval quality control because those waveforms were
8 susceptible to noise contamination. Shots during leaf-off season (November to March) were also
9 filtered out over deciduous forests and mixed forests. LAI and its profiles (0.15 m at vertical
10 resolution) were initially calculated for GLAS footprints based on a Geometric Optical and
11 Radiative Transfer (GORT) model (Ni-Meister et al., 2001), and further corrected for slope
12 effects using an iterative method (Tang et al., 2014a). Canopy VFP were calculated from
13 integration of footprint level LAI profiles at height intervals of 0 to 5 m, 5 to 10 m, 10 to 15 m
14 and 15 to 20 m. [More details of the GLAS data processing can be found in the supplement.](#)

15 **2.3 Comparison Data Sets**

16 We validated LAI and VFP data sets using an airborne lidar system, LVIS (Laser Vegetation
17 Imaging Sensor). LVIS is a medium resolution (~ 25 m diameter) waveform scanning lidar
18 system designed by NASA Goddard Space Flight Center (GSFC) (Blair et al., 1999). It can image
19 the terrestrial surface across a 2 km wide swath and has been deployed to map many different
20 forest structural parameters at regional scales across diverse biomes (Tang et al., 2012; Drake et
21 al., 2002; Swatantran et al., 2012). We calculated both total LAI and VFP at 5 m height intervals
22 from existing LVIS data using our physically based model, which has been validated using
23 different types of field measurements (destructive sampling, LAI-2000 and hemispherical photos)
24 (Tang et al., 2012; Tang et al., 2014a; Zhao et al., 2013). LVIS data used in this study included
25 major forest types from eastern, central and western US, including Maine forests just north of
26 Orono, Maine (2003), Sierra National Forest in California (2008), mixed forests along
27 Baltimore/Washington corridor (2003) and the White River National Wildlife Refuge in Arkansas
28 (2006). These LVIS datasets were all collected during leaf-on season.

1 We also included a 30 m resolution Landsat LAI map to examine the spatial distribution of
2 GLAS total LAI. Landsat has the longest earth observation history at moderate resolution (30 m),
3 and for decades has provided a consistent and unique measurement of terrestrial ecosystems. The
4 Landsat LAI map was produced using Global Land Survey (GLS) 2005 orthorectified Landsat
5 data (Ganguly et al., 2012; [Ganguly et al., In Prep.](#)).

6 **2.4 Analysis**

7 The comparison between LVIS and GLAS was performed at the GLAS footprint level. LVIS
8 shots falling within a 32.5 m radius from a GLAS shot center were selected. We filtered GLAS
9 footprints to have a minimum of 3 coincident LVIS shots to increase the likelihood that the LVIS
10 data covered a sufficient portion of the larger GLAS footprints. Both LAI and the 5 m interval
11 VFP of LVIS shots were averaged onto each coincident GLAS footprint for comparison. We also
12 made a footprint level comparison between GLAS LAI and the Landsat LAI map. A 3×3
13 [Landsat](#) window was applied to each GLAS footprint center to extract the averaged Landsat LAI
14 pixels. Pixels with invalid values (e.g. retrieval failure or non-vegetation pixel) were excluded in
15 the comparison. Agreements of different LAI datasets were assessed by coefficient of
16 determination, bias and RMSE (Root Mean Square Error):

$$17 \quad bias = \sum_{i=1}^n \frac{GLAS_i - Ref_i}{n} \quad (1)$$

$$18 \quad RMSE = \sqrt{\frac{\sum_{i=1}^n (GLAS_i - Ref_i)^2}{n}} \quad (2)$$

19 In Eq. (1) and Eq. (2), $GLAS_i$ is GLAS LAI (or VFP) value at footprint level and Ref_i is that
20 extracted from LVIS or Landsat.

21 Next, we aggregated the footprint level GLAS data into terrestrial ecoregions based on subset of a
22 global map (Olson et al., 2001). Statistical analysis of total LAI and LAI strata (VFP aggregated
23 at every 10 m height interval) was performed subsequently for each ecoregion. We also analyzed
24 the GLAS LAI and VFP distribution across different environmental gradients throughout
25 CONUS. GLAS footprints were categorized according to different environmental factors,
26 including vegetation type, topographic data and annual measurements of climate variables. The
27 vegetation map was derived from the MODIS Land Cover Type product (MCD12Q1) at 500 m

1 resolution following the IGBP scheme (Friedl et al., 2010). Elevation data was extracted from the
2 void-filled 90 m resolution SRTM (Shuttle Radar Topography Mission) DEM data (Reuter et al.,
3 2007). Precipitation, temperature and vapor pressure deficit information originated from the 800
4 m resolution 30yr annual normal climate data developed by the PRISM Climate Group (PRISM,
5 2013).

6 **3 Results**

7 This section includes three major parts: the first part focuses on the validation and comparison of
8 GLAS LAI and VFP data with existing products; the second presents the geographical
9 distribution of GLAS LAI and VFP, and; the last part shows their relationship with
10 environmental factors.

11 **3.1 GLAS LAI and VFP Comparisons with LVIS and Landsat**

12 The footprint level comparison between GLAS LAI and LVIS LAI had an overall r^2 of 0.60, bias
13 of -0.23, and RMSE of 0.82 (Fig. 1). Except for a few outliers at the lower range of LAI, most of
14 the comparison points were distributed along the 1:1 line suggesting no systematic difference
15 between the two data sets. No significant bias was found across individual sites either.

16 The agreement of the 5 m height interval VFP distributions between the two data sets was lower
17 than that of total LAI ($r^2 = 0.36$, a bias = -0.04 and RMSE = 0.26). Although there was no
18 systematic bias observed when all sites and vertical intervals are considered (Fig. 2), examination
19 by layer showed that GLAS overestimated understory LAI (0 to 5 m) ($r^2 = 0.04$, bias =
20 0.09, RMSE = 0.31) when compared with LVIS LAI (Fig. 3) but agreement improved as the
21 vertical height interval considered moved higher in the canopy (5 to 10 m, $r^2 = 0.33$, bias = -
22 0.13, RMSE = 0.29; and 10 to 15 m, $r^2 = 0.53$, bias = -0.08, RMSE = 0.22), reaching a maximum
23 at the top of the canopy (15 to 20 m, $r^2 = 0.66$, bias = -0.05, RMSE = 0.20).

24 The comparison between Landsat LAI and GLAS LAI had a much lower agreement than that of
25 LVIS ($r^2 = 0.18$, bias = 0.18 and RMSE = 2.02) (Fig. 4). Even though the two data sets agreed
26 well at lower LAI values, Landsat overestimated LAI at the middle range (from LAI values of 1
27 to 3) and then saturated above a value of about 4 to 5 against GLAS data.

1 **3.2 Aggregated GLAS LAI and VFP within Ecoregions**

2 We next mapped GLAS LAI across US ecoregions (Fig. 5). Highest LAI values were found along
3 northern Pacific Coast while lowest values occurred in the basin and range province and the arid
4 rains shadow region east of the Rocky Mountains. Northern California coastal forests (Pacific
5 temperate rainforests) were found to have the highest mean LAI value of 5.24. In the eastern
6 U.S., the mixed deciduous forests of the Appalachian-Blue Ridge province had the highest value
7 of 3.95 while other ecoregions around north-south direction of Appalachian Mountains had
8 similar LAI values around 3 ~ 4 (Table 1). Forest ecoregions with lowest LAI values (excluding
9 desert, shrubland and grassland) were located in Arizona mountains forests (1.15) and Great
10 Basin montane forests (0.90). Differences between these ecoregion-level LAI were significant
11 based on a bonferroni adjusted t-test, except for those among Willamette Valley forests,
12 Appalachian-Blue Ridge forests, Puget lowland forests and Appalachian mixed mesophytic
13 forests (p-values > 0.05).

14 LAI strata formed by VFP at each 10 m height interval were also averaged and mapped across the
15 US (Fig. 6). We chose the 10 m height interval rather than that of 5 m because LAI strata
16 aggregated at 10 m height interval represented a more accurate and reliable description of vertical
17 canopy structure given the relatively lower measurement accuracy in the understory (< 5 m) we
18 found in comparison to LVIS data. Each strata showed a generally similar geographic pattern as
19 that of total LAI with the decreasing trend from coast to interior lands, but the specific patterns
20 among strata differed. Northwestern forests were observed to have the highest total LAI values as
21 well as LAI strata values. Northern California coastal forests exhibited the largest total LAI value
22 as well as highest foliage density under 20 m height, while British Columbia mainland coastal
23 forests showed the highest foliage density (1.13) above 20 m height with a lower total LAI value
24 (4.74).

25 The distribution of GLAS total LAI and profiles were examined across different land cover types
26 (Fig. 7 and Fig. 8). Not surprisingly, forests were found to have a consistently greater value than
27 non-forest biomes in both total LAI and its strata. For example, deciduous broadleaf forests had
28 the highest value of total LAI (mean = 4.03) as well as that of middle and upper LAI strata
29 (height > 10 m), while open shrubland showed the lowest total LAI values of 0.77. However,
30 vertical LAI distributions of most forests and non-forests were similar with peak foliage density

1 distributed around a height of 2 ~ 4 m. The only exception was deciduous broadleaf forest, of
2 which most of leaves were distributed at middle-story level with a peak height at about 8 m. Its
3 VFP values did not decrease significantly until reaching a height of 15 m.

4 **3.3 GLAS LAI Distributions by Environmental Factors**

5 A linear regression analysis between GLAS LAI and SRTM DEM showed that increasing altitude
6 led to an overall decreasing, but non-monotonic, trend in LAI values ($LAI = 3.60 - 0.686 \times$
7 $Elevation (km)$, $r^2 = 0.59$, all $P < 0.01$) (Fig. 9). GLAS LAI values increased with DEM at the
8 elevation range from 0 to 750 m and 2000 to 3000 m. The variation in the LAI-DEM relationship
9 agreed well with Forest Ratio ($LAI = 0.112 + 3.18 \times Forest Ratio$, $r^2 = 0.45$, $P < 0.01$). Here each
10 GLAS footprint was classified as either forest or non-forest with an overlay of MODIS land cover
11 map, and the Forest Ratio was defined as the percentage of footprints classified as forests in total
12 GLAS shots within each elevation group~~Forest Ratio was, defined as the percentage of footprints~~
13 ~~classified as forests in total GLAS shots (forest and non-forest)~~. A multiple linear regression
14 analysis showed that about 87% of total variance could be explained by a simple combination of
15 elevation groups and Forest Ratio values: $LAI = 2.59 \times Forest Ratio - 0.595 \times Elevation (km) +$
16 1.58 .

17 We also analyzed GLAS LAI by 30yr normal annual climate data using linear regression models
18 (Fig. 10). It was observed that increasing precipitation significantly increased LAI values (ΔLAI
19 $= 1.84$ per 1000 mm precipitation increase) but only at low and moderate precipitation levels ($<$
20 2400 mm): $LAI = 1.84 \times precipitation (mm) \times 10^{-3} + 0.774$, $r^2 = 0.96$, $adj-r^2 = 0.95$, $P < 0.01$. It
21 contributed little when exceeding that threshold ($LAI = 0.22 \times precipitation (mm) \times 10^{-3}$, $r^2 =$
22 0.40 , $adj-r^2 = 0.30$, $P = 0.09$), as we found no significant LAI increase among groups greater
23 than 2400 mm using a bonferroni adjusted t-test. GLAS LAI was also negatively but slightly
24 correlated with minimum (maximum) vapor pressure deficit with a Pearson's correlation
25 coefficient of -0.29 (-0.15). The correlation coefficients between GLAS LAI and annual mean /
26 minimum / maximum temperature were even lower with values of 0.13, 0.18 and 0.08
27 respectively.

28 Finally, we applied multiple linear regression analysis to illustrate the combined environmental
29 effects of altitude and precipitation the on distributions of LAI and VFP. The regression analyses

1 were conducted at both GLAS footprint level and aggregated scale on altitude and precipitation
2 groups. At footprint level, altitude and precipitation together explained about 30% of variance of
3 total LAI ($LAI = 2.73 - 0.69 \times \text{Elevation (km)} + 0.58 \times \text{precipitation (mm)} \times 10^{-3}$, $r^2 = 0.29$, adj -
4 $r^2 = 0.29$, $P < 0.01$). However, their correlations with footprint level VFP (0 - 10 m, 10 - 20 m
5 and > 20 m height intervals) were not significant with r^2 of 0.07, 0.12 and 0.08 respectively. At
6 the aggregated scale, there was a better relationship between averaged LAI (VFP) values and
7 environmental factors. The combination of altitude and precipitation can explain more than 60%
8 variance in both total LAI and VFP, but explains only about 36% of variance on LAI for canopies
9 less than 10 m height.

10 **4 Discussion**

11 In this study, we generated GLAS estimates of LAI and VFP across the United States, validated
12 with an airborne lidar sensor, LVIS. Comparisons between LVIS and GLAS LAI and VFP
13 estimates in different forest types across the United States show that GLAS generally provides
14 accurate LAI and VFP estimates at footprint level. Considering the temporal offset and spatial
15 resolution differences between LVIS and GLAS, their overall agreements on LAI and VFP are
16 ~~reasonable-acceptable~~ ($r^2 = 0.60$, bias = -0.23, and RMSE = 0.82; and $r^2 = 0.36$, bias = -0.043,
17 and RMSE = 0.26). Our comparisons further demonstrate the efficacy of our retrieval methods
18 over continental scales that encompass large gradients in environmental factors and variability in
19 forest types.

20 Measurement accuracy of GLAS VFP was lower compared to total LAI but ($r^2 = 0.36$, bias = -
21 0.043, and RMSE = 0.26). Accuracies decreased for the lowest canopy layers, with the r^2 values
22 falling from a peak of 0.66 at upper-story (15 to 20 m) to 0.33 at middle-story (5 to 10 m), to
23 essentially no relationship in the lowest 5 meters in the understory. There may be multiple factors
24 contributing to this trend. First, a slope effect may reduce measurement accuracy of GLAS (Tang
25 et al., 2014a). Slopes can blur the boundary between vegetation and topography signals in a lidar
26 waveform, making their separation difficult and potentially leading to the error in LAI and VFP
27 estimates. Despite methods to correct for topography (Lee et al., 2011; Tang et al., 2014a; Park et
28 al., 2014), this effect cannot be fully mitigated, especially over steep slopes, and consequently
29 may introduce errors and uncertainties into VFP estimates. Additionally, topographical effects
30 can lead to a vertical misalignment of VFP between LVIS and GLAS. GLAS measures the

1 terrestrial surface at a larger footprint with higher topographical variations, and a direct average
2 of LVIS VFP can possibly result in a mismatch of vertical foliage distribution up to several
3 meters. For example, consider two adjacent LVIS shots with the same VFP distribution but a 1 m
4 difference in ground elevation (like a signal lag in the waveform). Adding the two waveforms
5 along the geodetic altitude would lead to a 1 m vertical offset in the averaged waveform (pseudo-
6 GLAS waveform) and produce a different VFP using the direct average method in a normalized
7 coordinate system. But their total LAI values remain the same as long as the total energy from
8 ground and vegetation can be separately correctly. Reducing vertical resolution of VFP can
9 partially mitigate the mismatch effect because a lower vertical resolution requires integration over
10 longer vertical axis which is more tolerant to ground mismatch. Take the above example again,
11 the two VFP, at 1 m vertical resolution, do not match each other at all along the entire waveform
12 due to the offset. However, integration at every 5 m creates a signal overlap of 4 m in each height
13 bin with a maximum of 20% measurement error. Thus there is ultimately a tradeoff between
14 vertical resolution and VFP accuracy. It also explains the higher agreement of total LAI
15 (essentially an integration of VFP over the entire canopy) in the comparison between LVIS and
16 GLAS. Lastly, measurement of near-ground understory vegetation by GLAS is difficult. By
17 default GLAS waveforms are processed by a Gaussian decomposition method to get an
18 approximate fit comprised of a series of Gaussian functions where the last one usually represents
19 the ground (Hofton et al., 2000). The upper tail of the ground Gaussian peak may be mixed with
20 signals from lower understory, and their separation is problematic, especially over slopes. All of
21 these factors, plus the nature of high complexity and heterogeneity in canopy understory (Aubin
22 et al., 2000; Valladares and Niinemets, 2008), may help explain the lower agreement on
23 understory VFP between LVIS and GLAS.

24 Comparison between GLAS and Landsat displayed a much lower agreement than that of LVIS,
25 was somewhat biased, and showed clear signals of saturation beyond LAI values of about 5. This
26 result, along with all previous studies (Tang et al., 2012; Tang et al., 2014b), clearly showed the
27 non-saturation advantage of lidar data against passive remote sensing in observing high LAI
28 forests. On the low end of LAI spectrum, GLAS values were lower as compared with Landsat.
29 There are different factors (some in the LVIS comparison too) could possibly lead to their
30 difference in LAI estimates such as geolocation errors of GLAS shots, observation scale

1 difference (65 m vs. 30 m) and misclassifications from MODIS land cover types (mainly
2 impacting the correction of clumping effect). But this underestimation should be largely due to
3 the fact that GLAS may not be able to adequately capture LAI values of short grassland with
4 limited vertical structure or areas of sparse canopy cover, whereas Landsat is able measure such
5 areas based on their total spectral response (tree and grass).

6 Analysis of GLAS LAI and VFP across ecoregions displayed a reasonable and expected
7 geographical distribution. The great advantage of lidar based estimates is that they can produce
8 LAI vertical strata maps, providing a view of canopy variability across ecosystem types over
9 large areas. Specifically, we can identify the foliage concentrations at various vertical bins and at
10 spatial resolutions of interest (Fig. 6, Fig. 8 and Table 1; [another example provided in the](#)
11 [supplement](#)). This approach may reduce errors that arise from assumptions of uniformly
12 distributed foliage within canopy, and could potentially be a contribution towards continental
13 scale ecological and biological studies of forest structure and dynamics.

14 LAI and VFP also varied across different landscapes represented by various land cover types. As
15 expected, we found both total LAI and maximum value of foliage density significantly increase
16 along the vegetation gradient described by the transition from shrubland to savanna to woody
17 savanna to forests (Fig. 7 and Fig. 8). In particular, we found deciduous broadleaf forest showing
18 a different pattern with its foliage more evenly distributed in understory and mid-story when
19 compared with all other forests. Our results suggest the existence of canopy layering, and
20 highlight the feasibility of quantifying these layers across landscapes (Whitehurst et al., 2013).
21 Regardless, of whether the data are conceptualized as layers or as continuously varying profiles,
22 they nonetheless provide the actual vertical structure, and thus should help refine current
23 empirical assumptions about vegetation structure of different land cover types in current LAI
24 inversion algorithms (e.g. MODIS) and in ecosystem models (Hurt et al., 2010; Antonarakis et
25 al., 2014).

26 Elevation and precipitation were found to be significantly correlated with LAI at both footprint
27 level and across aggregated groupings by elevation and forest ratio. LAI decreased with elevation
28 and this trend was consistent with previous studies (Luo et al., 2004; Moser et al., 2007; Pfeifer et
29 al., 2012). Variations of the trend can be largely explained (about 45 % of total variance) by the
30 Forest Ratio (defined in Sect. 3.3). A combination of the two factors (elevation groups and Forest

1 Ratio) explained almost 90% variance of average LAI spatial distribution. We also found a
2 significant but nonlinear relationship between GLAS LAI and annual precipitation (Fig. 10). This
3 non-linear relationship agrees with previous studies in the tropics (Pfeifer et al., 2014;Spracklen
4 et al., 2012). However, we found no significant variation of GLAS LAI with either temperature or
5 vapor pressure deficit variables. A combined effect of elevation and precipitation explains about
6 30% of LAI variation at GLAS footprint level, suggesting the natural complexity highly spatial
7 variability of LAI distribution.

8 As a direct quantification of 3D foliage distribution, GLAS LAI profiles are thus far the best
9 representations of terrestrial ecosystem structure over broad geographical areas and suggest that
10 ecological applications of these profiles are worth exploring. First, this data could refine large
11 scale modeling of plant respiration and photosynthesis and consequently and improve ecosystem
12 modeling (Houghton, 2007). Previous studies have reported a potential 50% underestimate of
13 GPP values when vertical foliage stratification is not considered (Kotchenova et al.,
14 2004;Sprintsin et al., 2012). A consistent, global data set of VFP should thus improve
15 initialization of ecological models (Hurtt et al., 2004), and refine estimation of GPP, in
16 conjunction with passive remote sensing data (Turner et al., 2006). Secondly, these profiles may
17 be important descriptors of habitat as related to biodiversity and habitat quality. Many studies
18 have confirmed the general relationship between species richness, habitat heterogeneity and
19 forest structural complexity across different landscapes (Swatantran et al., 2012;Goetz et al.,
20 2010;Schut et al., 2014;Ferber et al., 2014). The inclusion of LAI profiles provides spatially
21 explicit vegetation structure data and may potentially improve current observations of species
22 distribution at continental scale, e.g. for avian species (Sauer et al., 2008;Culbert et al., 2013), and
23 lead to entirely new biodiversity metrics (e.g. see (Huang et al., 2014)). For example the concept
24 of an "edge" has been traditionally defined as the boundary between forest and non-forest areas.
25 LAI profiles provide a means of defining new edges based on differences in LAI as a function of
26 height, so the edge is now the boundary between a rapid change in foliage density at a particular
27 height.

28

1 **5 Conclusion**

2 Accurate representation of canopy vertical structure and its dynamics has long been recognized as
3 a priority because it represents a key interface between terrestrial surface and atmosphere and
4 impacts the water and carbon cycles, and their transfer of energy and mass. Foliar profiles are
5 also increasingly recognized as important determinants for habitat quality, species distribution,
6 diversity and abundance. As ecosystems come under increasing pressure from climate and land
7 use change, global data sets of canopy structure are needed to help better understand the
8 consequences of these changes on ecosystem form, function and services.

9 In this paper we have demonstrated the potential for global mapping of key canopy structures,
10 LAI and VFP, from space. While imperfect, given their large footprint and sparse sampling, the
11 waveforms from ICESat are currently the only such global data set of structure. Our ability to
12 produce this data set is the end result of a series of research experiments that linked various types
13 of observations, from destructive profiles, to ground based optical methods, to airborne lidar, to
14 passive optical retrievals. This background gives us confidence that meaningful and useful data
15 on LAI and VFP can be derived from future spaceborne lidar. There are still hurdles to overcome
16 related to topography, understory accuracy, model assumptions and parameterizations, such as
17 ground/canopy reflectance ratios and foliage clumping, among others, to achieving higher
18 accuracy. We anticipate these will be resolved in time and lead to an even more capable model
19 suitable for the next generation of waveform lidar observations from space, such as NASA's
20 Global Ecosystem Dynamics Investigation (GEDI) (Dubayah et al., 2014) and potentially
21 ICESat-2 (Abdalati et al., 2009).

22

23 **Acknowledgements**

24 This work was funded by NASA under grant NNX12AK07G (Dubayah) and an Earth and Space
25 Science graduate fellowship NNX12AN43H (Dubayah/Tang). We thank Helen G. Cornejo and
26 Wenli Huang for raw LVIS waveform process, George Hurtt and Shunlin Liang for their advice
27 on product development. We also thank the NSIDC (National Snow & Ice Data Center) User
28 Services for their help on data acquisition and NASA Earth Exchange (NEX) for computing
29 resources.

1 **References**

- 2 Abdalati, W., Zwally, H. J., Bindschadler, R., Csatho, B., Farrell, S. L., Fricker, H. A., Harding,
3 D., Kwok, R., Lefsky, M., Markus, T., Marshak, A., Neumann, T., Palm, S., Schutz, B., Smith,
4 B., Spinhirne, J., and Webb, C.: The ICESat-2 laser altimetry mission, *Proceedings of the IEEE*,
5 98, 735-751, 2009.
- 6 Aber, J. D.: Foliage-height profiles and succession in northern hardwood forests, *Ecology*, 60,
7 18-23, 1979.
- 8 Abshire, J. B., Sun, X., Riris, H., Sirota, J. M., McGarry, J. F., Palm, S., Yi, D., and Liiva, P.:
9 Geoscience Laser Altimeter System (GLAS) on the icesat mission: On-orbit measurement
10 performance, *Geophysical Research Letters*, 32, L21S02, doi:10.1029/2005GL024028, 2005.
- 11 Abuelgasim, A. A., Fernandes, R. A., and Leblanc, S. G.: Evaluation of national and global lai
12 products derived from optical remote sensing instruments over canada, *IEEE Transactions on*
13 *Geoscience and Remote Sensing*, 44, 1872-1884, Doi 10.1109/Tgrs.2006.874794, 2006.
- 14 Antonarakis, A. S., Munger, J. W., and Moorcroft, P. R.: Imaging spectroscopy- and lidar-derived
15 estimates of canopy composition and structure to improve predictions of forest carbon fluxes and
16 ecosystem dynamics, *Geophysical Research Letters*, 41, 2535-2542, Doi 10.1002/2013gl058373,
17 2014.
- 18 Asner, G. P., Knapp, D. E., Boardman, J., Green, R. O., Kennedy-Bowdoin, T., Eastwood, M.,
19 Martin, R. E., Anderson, C., and Field, C. B.: Carnegie airborne observatory-2: Increasing
20 science data dimensionality via high-fidelity multi-sensor fusion, *Remote Sensing of*
21 *Environment*, 124, 454-465, DOI 10.1016/j.rse.2012.06.012, 2012.
- 22 Asner, G. P., Mascaro, J., Anderson, C., Knapp, D. E., Martin, R. E., Kennedy-Bowdoin, T., van
23 Breugel, M., Davies, S., Hall, J. S., Muller-Landau, H. C., Potvin, C., Sousa, W., Wright, J., and
24 Birmingham, E.: High-fidelity national carbon mapping for resource management and redd+,
25 *Carbon Balance and Management*, 8, 7, doi:10.1186/1750-0680-8-7, 2013.
- 26 Aubin, I., Beaudet, M., and Messier, C.: Light extinction coefficients specific to the understory
27 vegetation of the southern boreal forest, quebec, *Canadian Journal of Forest Research-Revue*
28 *Canadienne De Recherche Forestiere*, 30, 168-177, DOI 10.1139/cjfr-30-1-168, 2000.

1 Baccini, A., Goetz, S. J., Walker, W. S., Laporte, N. T., Sun, M., Sulla-Menashe, D., Hackler, J.,
2 Beck, P. S. A., Dubayah, R., Friedl, M. A., Samanta, S., and Houghton, R. A.: Estimated carbon
3 dioxide emissions from tropical deforestation improved by carbon-density maps, *Nature Climate*
4 *Change*, 2, 182-185, Doi 10.1038/Nclimate1354, 2012.

5 Baret, F., Hagolle, O., Geiger, B., Bicheron, P., Miras, B., Huc, M., Berthelot, B., Nino, F.,
6 Weiss, M., Samain, O., Roujean, J. L., and Leroy, M.: Lai, fapar and fcover cyclopes global
7 products derived from vegetation - part 1: Principles of the algorithm, *Remote Sensing of*
8 *Environment*, 110, 275-286, DOI 10.1016/j.rse.2007.02.018, 2007.

9 Baret, F., Weiss, M., Lacaze, R., Camacho, F., Makhmara, H., Pacholczyk, P., and Smets, B.:
10 Geov1: Lai and fapar essential climate variables and fcover global time series capitalizing over
11 existing products. Part1: Principles of development and production, *Remote Sensing of*
12 *Environment*, 137, 299-309, DOI 10.1016/j.rse.2012.12.027, 2013.

13 Blair, J. B., Rabine, D. L., and Hofton, M. A.: The laser vegetation imaging sensor (LVIS): A
14 medium-altitude, digitization-only, airborne laser altimeter for mapping vegetation and
15 topography, *ISPRS journal of photogrammetry and remote sensing*, 54, 115-122, 1999.

16 Brenner, A. C., Zwally, H. J., Bentley, C. R., Csatho, B. M., Harding, D. J., Hofton, M. A.,
17 Minster, J.-B., Roberts, L., Saba, J. L., and Thomas, R. H.: The algorithm theoretical basis
18 document for the derivation of range and range distributions from laser pulse waveform analysis
19 for surface elevations, roughness, slope, and vegetation heights, Goddard Space Flight Center,
20 Greenbelt, MD, United States, Technical Report NASA/TM-2012-208641/Vol 7,
21 GSFC.TM.7299.2012, 2012.

22 Chopping, M., Nolin, A., Moisen, G. G., Martonchik, J. V., and Bull, M.: Forest canopy height
23 from the multiangle imaging spectroradiometer (MISR) assessed with high resolution discrete
24 return lidar, *Remote Sensing of Environment*, 113, 2172-2185, DOI 10.1016/j.rse.2009.05.017,
25 2009.

26 Clark, D. B., and Kellner, J. R.: Tropical forest biomass estimation and the fallacy of misplaced
27 concreteness, *Journal of Vegetation Science*, 23, 1191-1196, DOI 10.1111/j.1654-
28 1103.2012.01471.x, 2012.

1 Cramer, W., Bondeau, A., Woodward, F. I., Prentice, I. C., Betts, R. A., Brovkin, V., Cox, P. M.,
2 Fisher, V., Foley, J. A., Friend, A. D., Kucharik, C., Lomas, M. R., Ramankutty, N., Sitch, S.,
3 Smith, B., White, A., and Young-Molling, C.: Global response of terrestrial ecosystem structure
4 and function to co₂ and climate change: Results from six dynamic global vegetation models,
5 *Global Change Biology*, 7, 357-373, DOI 10.1046/j.1365-2486.2001.00383.x, 2001.

6 Culbert, P. D., Radeloff, V. C., Flather, C. H., Kellndorfer, J. M., Rittenhouse, C. D., and
7 Pidgeon, A. M.: The influence of vertical and horizontal habitat structure on nationwide patterns
8 of avian biodiversity, *Auk*, 130, 656-665, DOI 10.1525/auk.2013.13007, 2013.

9 Deng, F., Chen, J. M., Plummer, S., Chen, M. Z., and Pisek, J.: Algorithm for global leaf area
10 index retrieval using satellite imagery, *IEEE Transactions on Geoscience and Remote Sensing*,
11 44, 2219-2229, Doi 10.1109/Tgrs.2006.872100, 2006.

12 Drake, J. B., Dubayah, R. O., Clark, D. B., Knox, R. G., Blair, J. B., Hofton, M. A., Chazdon, R.
13 L., Weishampel, J. F., and Prince, S. D.: Estimation of tropical forest structural characteristics
14 using large-footprint lidar, *Remote Sensing of Environment*, 79, 305-319, Doi 10.1016/S0034-
15 4257(01)00281-4, 2002.

16 Dubayah, R., Bergen, K., Hall, F., Hurtt, G., Houghton, R., Kellndorfer, J., Lefsky, M.,
17 Moorcroft, P., Nelson, R., and Saatchi, S.: Global vegetation structure from nasa's desdyni
18 mission: An overview, *AGU Fall Meeting Abstracts*, 01, San Francisco, 15 December, B31H- 01,
19 2008.

20 Dubayah, R., Goetz, S., Blair, J. B., Fatoyinbo, T., Hansen, M., Healey, S., Hofton, M., Hurtt, G.,
21 Kellner, J. R., Luthcke, S. B., and Swatantran, A.: The global ecosystem dynamics investigation,
22 *American Geophysical Union, Fall Meeting 2014*, San Francisco, 15 December, U14A-07, 2014.

23 Ferger, S. W., Schleuning, M., Hemp, A., Howell, K. M., and Böhning-Gaese, K.: Food resources
24 and vegetation structure mediate climatic effects on species richness of birds, *Global Ecology and*
25 *Biogeography*, 23, 541-549, 10.1111/geb.12151, 2014.

26 Friedl, M. A., Sulla-Menashe, D., Tan, B., Schneider, A., Ramankutty, N., Sibley, A., and Huang,
27 X. M.: Modis collection 5 global land cover: Algorithm refinements and characterization of new
28 datasets, *Remote Sensing of Environment*, 114, 168-182, DOI 10.1016/j.rse.2009.08.016, 2010.

1 [Ganguly, S., et al. : Generating leaf area index from landsat over the Unites States. Manuscript in](#)
2 [preparation.](#)

3 Ganguly, S., Nemani, R. R., Zhang, G., Hashimoto, H., Milesi, C., Michaelis, A., Wang, W. L.,
4 Votava, P., Samanta, A., Melton, F., Dungan, J. L., Vermote, E., Gao, F., Knyazikhin, Y., and
5 Myneni, R. B.: Generating global leaf area index from landsat: Algorithm formulation and
6 demonstration, *Remote Sensing of Environment*, 122, 185-202, DOI 10.1016/j.rse.2011.10.032,
7 2012.

8 Garcia, M., Popescu, S., Riano, D., Zhao, K., Neuenschwander, A., Agca, M., and Chuvieco, E.:
9 Characterization of canopy fuels using ICESat/GLAS data, *Remote Sensing of Environment*, 123,
10 81-89, 10.1016/j.rse.2012.03.018, 2012.

11 Goetz, S., Steinberg, D., Dubayah, R., and Blair, B.: Laser remote sensing of canopy habitat
12 heterogeneity as a predictor of bird species richness in an eastern temperate forest, USA, *Remote*
13 *Sensing of Environment*, 108, 254-263, DOI 10.1016/j.rse.2006.11.016, 2007.

14 Goetz, S. J., Steinberg, D., Betts, M. G., Holmes, R. T., Doran, P. J., Dubayah, R., and Hofton,
15 M.: Lidar remote sensing variables predict breeding habitat of a neotropical migrant bird,
16 *Ecology*, 91, 1569-1576, Doi 10.1890/09-1670.1, 2010.

17 Gower, S. T., and Norman, J. M.: Rapid estimation of leaf area index in conifer and broad-leaf
18 plantations, *Ecology*, 72, 1896-1900, 1991.

19 Harding, D. J., and Carabajal, C. C.: ICESat waveform measurements of within-footprint
20 topographic relief and vegetation vertical structure, *Geophysical Research Letters*, 32, Artn
21 L21s10, Doi 10.1029/2005gl023471, 2005.

22 Healey, S. P., Patterson, P. L., Saatchi, S., Lefsky, M. A., Lister, A. J., and Freeman, E. A.: A
23 sample design for globally consistent biomass estimation using lidar data from the Geoscience
24 Laser Altimeter System (GLAS), *Carbon Balance and Management*, 7, 10, doi:10.1186/1750-
25 0680-7-10, 2012.

26 Heimann, M., and Reichstein, M.: Terrestrial ecosystem carbon dynamics and climate feedbacks,
27 *Nature*, 451, 289-292, Doi 10.1038/Nature06591, 2008.

1 Hofton, M. A., Minster, J. B., and Blair, J. B.: Decomposition of laser altimeter waveforms, IEEE
2 Transactions on Geoscience and Remote Sensing, 38, 1989-1996, 2000.

3 Houghton, R. A.: Balancing the global carbon budget, Annual Review of Earth and Planetary
4 Sciences, 35, 313-347, DOI 10.1146/annurev.earth.35.031306.140057, 2007.

5 Huang, Q. Y., Swatantran, A., Dubayah, R., and Goetz, S. J.: The influence of vegetation height
6 heterogeneity on forest and woodland bird species richness across the united states, Plos One, 9,
7 ARTN e103236, DOI 10.1371/journal.pone.0103236, 2014.

8 Hurtt, G. C., Dubayah, R., Drake, J., Moorcroft, P. R., Pacala, S. W., Blair, J. B., and Fearon, M.
9 G.: Beyond potential vegetation: Combining lidar data and a height-structured model for carbon
10 studies, Ecological Applications, 14, 873-883, 2004.

11 Hurtt, G. C., Fisk, J., Thomas, R. Q., Dubayah, R., Moorcroft, P. R., and Shugart, H. H.: Linking
12 models and data on vegetation structure, Journal of Geophysical Research-Biogeosciences, 115,
13 Artn G00e10, Doi 10.1029/2009jg000937, 2010.

14 Kotchenova, S. Y., Song, X. D., Shabanova, N. V., Potter, C. S., Knyazikhin, Y., and Myneni, R.
15 B.: Lidar remote sensing for modeling gross primary production of deciduous forests, Remote
16 Sensing of Environment, 92, 158–172, doi:10.1016/j.rse.2004.05.010, 2004.

17 Lee, S., Ni-Meister, W., Yang, W. Z., and Chen, Q.: Physically based vertical vegetation
18 structure retrieval from icesat data: Validation using LVIS in white mountain national forest, new
19 hampshire, USA, Remote Sensing of Environment, 115, 2776-2785, DOI
20 10.1016/j.rse.2010.08.026, 2011.

21 Lefsky, M. A., Cohen, W. B., Parker, G. G., and Harding, D. J.: Lidar remote sensing for
22 ecosystem studies, BioScience, 52, 19-19, 2002.

23 Lefsky, M. A.: A global forest canopy height map from the moderate resolution imaging
24 spectroradiometer and the geoscience laser altimeter system, Geophysical Research Letters, 37,
25 L15401, doi:10.1029/2010GL043622, 2010.

26 Loreau, M., Naeem, S., Inchausti, P., Bengtsson, J., Grime, J. P., Hector, A., Hooper, D. U.,
27 Huston, M. A., Raffaelli, D., Schmid, B., Tilman, D., and Wardle, D. A.: Ecology - biodiversity

1 and ecosystem functioning: Current knowledge and future challenges, *Science*, 294, 804-808,
2 DOI 10.1126/science.1064088, 2001.

3 Los, S. O., Rosette, J. A. B., Kljun, N., North, P. R. J., Chasmer, L., Suñez, J. C., Hopkinson,
4 C., Hill, R. A., van Gorsel, E., Mahoney, C., and Berni, J. A. J.: Vegetation height and cover
5 fraction between 60° s and 60° n from ICESat GLAS data, *Geosci. Model Dev.*, 5, 413-432,
6 10.5194/gmd-5-413-2012, 2012.

7 Luo, S. Z., Wang, C., Li, G. C., and Xi, X. H.: Retrieving leaf area index using icesat/glas full-
8 waveform data, *Remote Sensing Letters*, 4, 745-753, Doi 10.1080/2150704x.2013.790573, 2013.

9 Luo, T. X., Pan, Y. D., Ouyang, H., Shi, P. L., Luo, J., Yu, Z. L., and Lu, Q.: Leaf area index and
10 net primary productivity along subtropical to alpine gradients in the tibetan plateau, *Global
11 Ecology and Biogeography*, 13, 345-358, DOI 10.1111/j.1466-822X.2004.00094.x, 2004.

12 Morsdorf, F., Kotz, B., Meier, E., Itten, K., and Allgower, B.: Estimation of lai and fractional
13 cover from small footprint airborne laser scanning data based on gap fraction, *Remote Sensing of
14 Environment*, 104, 50-61, 2006.

15 Moser, G., Hertel, D., and Leuschner, C.: Altitudinal change in lai and stand leaf biomass in
16 tropical montane forests: A transect shady in ecuador and a pan-tropical meta-analysis,
17 *Ecosystems*, 10, 924-935, DOI 10.1007/s10021-007-9063-6, 2007.

18 Mu, Q., Heinsch, F. A., Zhao, M., and Running, S. W.: Development of a global
19 evapotranspiration algorithm based on modis and global meteorology data, *Remote Sensing of
20 Environment*, 111, 519-536, DOI 10.1016/j.rse.2007.04.015, 2007.

21 Myneni, R. B., Hoffman, S., Knyazikhin, Y., Privette, J. L., Glassy, J., Tian, Y., Wang, Y., Song,
22 X., Zhang, Y., Smith, G. R., Lotsch, A., Friedl, M., Morisette, J. T., Votava, P., Nemani, R. R.,
23 and Running, S. W.: Global products of vegetation leaf area and fraction absorbed par from year
24 one of modis data, *Remote Sensing of Environment*, 83, 214-231, Pii S0034-4257(02)00074-3
25 Doi 10.1016/S0034-4257(02)00074-3, 2002.

26 Ni-Meister, W., Jupp, D. L. B., and Dubayah, R.: Modeling lidar waveforms in heterogeneous
27 and discrete canopies, *IEEE Transactions on Geoscience and Remote Sensing*, 39, 1943-1958,
28 2001.

1 Nilson, T.: A theoretical analysis of the frequency of gaps in plant stands, *Agricultural*
2 *Meteorology*, 8, 25-38, 1971.

3 Olson, D. M., Dinerstein, E., Wikramanayake, E. D., Burgess, N. D., Powell, G. V. N.,
4 Underwood, E. C., D'amico, J. A., Itoua, I., Strand, H. E., Morrison, J. C., Loucks, C. J., Allnutt,
5 T. F., Ricketts, T. H., Kura, Y., Lamoreux, J. F., Wettengel, W. W., Hedao, P., and Kassem, K.
6 R.: Terrestrial ecoregions of the world: A new map of life on earth: A new global map of
7 terrestrial ecoregions provides an innovative tool for conserving biodiversity, *BioScience*, 51,
8 933-938, 10.1641/0006-3568(2001)051[0933:teotwa]2.0.co;2, 2001.

9 Park, T., Kennedy, R. E., Choi, S. H., Wu, J. W., Lefsky, M. A., Bi, J., Mantooth, J. A., Myneni,
10 R. B., and Knyazikhin, Y.: Application of physically-based slope correction for maximum forest
11 canopy height estimation using waveform lidar across different footprint sizes and locations:
12 Tests on lvis and glas, *Remote Sensing*, 6, 6566-6586, Doi 10.3390/Rs6076566, 2014.

13 Pereira, H. M., Ferrier, S., Walters, M., Geller, G. N., Jongman, R. H. G., Scholes, R. J., Bruford,
14 M. W., Brummitt, N., Butchart, S. H. M., Cardoso, A. C., Coops, N. C., Dulloo, E., Faith, D. P.,
15 Freyhof, J., Gregory, R. D., Heip, C., Hoft, R., Hurtt, G., Jetz, W., Karp, D. S., McGeoch, M. A.,
16 Obura, D., Onoda, Y., Pettorelli, N., Reyers, B., Sayre, R., Scharlemann, J. P. W., Stuart, S. N.,
17 Turak, E., Walpole, M., and Wegmann, M.: Essential biodiversity variables, *Science*, 339, 277-
18 278, DOI 10.1126/science.1229931, 2013.

19 Pfeifer, M., Gonsamo, A., Disney, M., Pellikka, P., and Marchant, R.: Leaf area index for biomes
20 of the eastern arc mountains: Landsat and spot observations along precipitation and altitude
21 gradients, *Remote Sensing of Environment*, 118, 103-115, DOI 10.1016/j.rse.2011.11.009, 2012.

22 Pfeifer, M., Lefebvre, V., Gonsamo, A., Pellikka, P., Marchant, R., Denu, D., and Platts, P.:
23 Validating and linking the gimms leaf area index (LAI3g) with environmental controls in tropical
24 africa, *Remote Sensing*, 6, 1973-1990, 2014.

25 PRISM: 30 yr normal precipitation: annual, in: 1981–2010, August 2013 ed., PRISM Climate
26 Group, Oregon State University, Corvallis, OR, 2013.

27 Randerson, J. T., Hoffman, F. M., Thornton, P. E., Mahowald, N. M., Lindsay, K., Lee, Y. H.,
28 Nevison, C. D., Doney, S. C., Bonan, G., Stockli, R., Covey, C., Running, S. W., and Fung, I. Y.:

1 Systematic assessment of terrestrial biogeochemistry in coupled climate-carbon models, *Global*
2 *Change Biology*, 15, 2462-2484, DOI 10.1111/j.1365-2486.2009.01912.x, 2009.

3 Reuter, H. I., Nelson, A., and Jarvis, A.: An evaluation of void-filling interpolation methods for
4 srtm data, *International Journal of Geographical Information Science*, 21, 983-1008, Doi
5 10.1080/13658810601169899, 2007.

6 Saatchi, S. S., Harris, N. L., Brown, S., Lefsky, M., Mitchard, E. T. A., Salas, W., Zutta, B. R.,
7 Buermann, W., Lewis, S. L., Hagen, S., Petrova, S., White, L., Silman, M., and Morel, A.:
8 Benchmark map of forest carbon stocks in tropical regions across three continents, *Proceedings*
9 *of the National Academy of Sciences of the United States of America*, 108, 9899-9904, DOI
10 10.1073/pnas.1019576108, 2011.

11 Sauer, J. R., Hines, J. E., Fallon, J., Pardieck, K., Ziolkowski Jr, D., and Link, W.: The north
12 american breeding bird survey, results and analysis 1966-2007, Version, 5, Laurel, MD, USGS
13 Patuxent Wildlife Research Center, 2008.

14 Schimel, D. S., House, J. I., Hibbard, K. A., Bousquet, P., Ciais, P., Peylin, P., Braswell, B. H.,
15 Apps, M. J., Baker, D., Bondeau, A., Canadell, J., Churkina, G., Cramer, W., Denning, A. S.,
16 Field, C. B., Friedlingstein, P., Goodale, C., Heimann, M., Houghton, R. A., Melillo, J. M.,
17 Moore, B., Murdiyarso, D., Noble, I., Pacala, S. W., Prentice, I. C., Raupach, M. R., Rayner, P.
18 J., Scholes, R. J., Steffen, W. L., and Wirth, C.: Recent patterns and mechanisms of carbon
19 exchange by terrestrial ecosystems, *Nature*, 414, 169-172, Doi 10.1038/35102500, 2001.

20 Schut, A. G. T., Wardell-Johnson, G. W., Yates, C. J., Keppel, G., Baran, I., Franklin, S. E.,
21 Hopper, S. D., Van Niel, K. P., Mucina, L., and Byrne, M.: Rapid characterisation of vegetation
22 structure to predict refugia and climate change impacts across a global biodiversity hotspot, *Plos*
23 *One*, 9, ARTN e82778, DOI 10.1371/journal.pone.0082778, 2014.

24 Shabanov, N. V., Huang, D., Yang, W. Z., Tan, B., Knyazikhin, Y., Myneni, R. B., Ahl, D. E.,
25 Gower, S. T., Huete, A. R., Aragao, L. E. O. C., and Shimabukuro, Y. E.: Analysis and
26 optimization of the modis leaf area index algorithm retrievals over broadleaf forests, *IEEE*
27 *Transactions on Geoscience and Remote Sensing*, 43, 1855-1865, Doi
28 10.1109/Tgrs.2005.852477, 2005.

1 Simard, M., Pinto, N., Fisher, J. B., and Baccini, A.: Mapping forest canopy height globally with
2 spaceborne lidar, *Journal of Geophysical Research-Biogeosciences*, 116, Artn G04021, Doi
3 10.1029/2011jg001708, 2011.

4 Spracklen, D. V., Arnold, S. R., and Taylor, C. M.: Observations of increased tropical rainfall
5 preceded by air passage over forests, *Nature*, 489, 282-U127, Doi 10.1038/Nature11390, 2012.

6 Sprintsin, M., Chen, J. M., Desai, A., and Gough, C. M.: Evaluation of leaf-to-canopy upscaling
7 methodologies against carbon flux data in north america, *Journal of Geophysical Research-*
8 *Biogeosciences*, 117, Artn G01023, Doi 10.1029/2010jg001407, 2012.

9 Stahl, G., Holm, S., Gregoire, T. G., Gobakken, T., Naesset, E., and Nelson, R.: Model-based
10 inference for biomass estimation in a lidar sample survey in hedmark county, norway, *Canadian*
11 *Journal of Forest Research-Revue Canadienne De Recherche Forestiere*, 41, 96-107, Doi
12 10.1139/X10-161, 2011.

13 Strahler, A. H., Jupp, D. L. B., Woodcock, C. E., Schaaf, C. B., Yao, T., Zhao, F., Yang, X.,
14 Lovell, J., Culvenor, D., Newnham, G., Ni-Miester, W., and Boykin-Morris, W.: Retrieval of
15 forest structural parameters using a ground-based lidar instrument (echidna®), *Canadian Journal*
16 *of Remote Sensing*, 34, S426–S440, doi:10.5589/m08-046, 2008.

17 Swatantran, A., Dubayah, R., Goetz, S., Hofton, M., Betts, M. G., Sun, M., Simard, M., and
18 Holmes, R.: Mapping migratory bird prevalence using remote sensing data fusion, *Plos One*, 7,
19 e28922, doi:10.1371/journal.pone.0028922, 2012.

20 Tang, H., Dubayah, R., Swatantran, A., Hofton, M., Sheldon, S., Clark, D. B., and Blair, B.:
21 Retrieval of vertical lai profiles over tropical rain forests using waveform lidar at la selva, costa
22 rica, *Remote Sensing of Environment*, 124, 242-250, 10.1016/j.rse.2012.05.005, 2012.

23 Tang, H., Brolly, M., Zhao, F., Strahler, A. H., Schaaf, C. L., Ganguly, S., Zhang, G., and
24 Dubayah, R.: Deriving and validating leaf area index (lai) at multiple spatial scales through lidar
25 remote sensing: A case study in sierra national forest, ca, *Remote Sensing of Environment*, 143,
26 131-141, 2014a.

1 Tang, H., Dubayah, R., Brolly, M., Ganguly, S., and Zhang, G.: Large-scale retrieval of leaf area
2 index and vertical foliage profile from the spaceborne waveform lidar (glas/icesat), *Remote*
3 *Sensing of Environment*, 154, 8-18, DOI 10.1016/j.rse.2014.08.007, 2014b.

4 Turner, D. P., Ritts, W. D., Cohen, W. B., Gower, S. T., Running, S. W., Zhao, M. S., Costa, M.
5 H., Kirschbaum, A. A., Ham, J. M., Saleska, S. R., and Ahl, D. E.: Evaluation of modis npp and
6 gpp products across multiple biomes, *Remote Sensing of Environment*, 102, 282-292, DOI
7 10.1016/j.rse.2006.02.017, 2006.

8 Turner, W., Spector, S., Gardiner, N., Fladeland, M., Sterling, E., and Steininger, M.: Remote
9 sensing for biodiversity science and conservation, *Trends in Ecology & Evolution*, 18, 306-314,
10 Doi 10.1016/S0169-5347(03)00070-3, 2003.

11 Valladares, F., and Niinemets, U.: Shade tolerance, a key plant feature of complex nature and
12 consequences, *Annual Review of Ecology Evolution and Systematics*, 39, 237-257, DOI
13 10.1146/annurev.ecolsys.39.110707.173506, 2008.

14 Whitehurst, A. S., Swatantran, A., Blair, J. B., Hofton, M. A., and Dubayah, R.: Characterization
15 of canopy layering in forested ecosystems using full waveform lidar, *Remote Sensing*, 5, 2014-
16 2036, Doi 10.3390/Rs5042014, 2013.

17 Yang, W. Z., Tan, B., Huang, D., Rautiainen, M., Shabanov, N. V., Wang, Y., Privette, J. L.,
18 Huemmrich, K. F., Fensholt, R., Sandholt, I., Weiss, M., Ahl, D. E., Gower, S. T., Nemani, R. R.,
19 Knyazikhin, Y., and Myneni, R. B.: Modis leaf area index products: From validation to algorithm
20 improvement, *IEEE Transactions on Geoscience and Remote Sensing*, 44, 1885-1898, Doi
21 10.1109/Tgrs.2006.871215, 2006.

22 Zhao, F., Yang, X. Y., Strahler, A. H., Schaaf, C. L., Yao, T., Wang, Z. S., Roman, M. O.,
23 Woodcock, C. E., Ni-Meister, W., Jupp, D. L. B., Lovell, J. L., Culvenor, D. S., Newnham, G. J.,
24 Tang, H., and Dubayah, R. O.: A comparison of foliage profiles in the sierra national forest
25 obtained with a full-waveform under-canopy evi lidar system with the foliage profiles obtained
26 with an airborne full-waveform lvis lidar system, *Remote Sensing of Environment*, 136, 330-341,
27 DOI 10.1016/j.rse.2013.05.020, 2013.

1 Zhao, M. S., Heinsch, F. A., Nemani, R. R., and Running, S. W.: Improvements of the modis
2 terrestrial gross and net primary production global data set, *Remote Sensing of Environment*, 95,
3 164-176, DOI 10.1016/j.rse.2004.12.011, 2005.

4

5

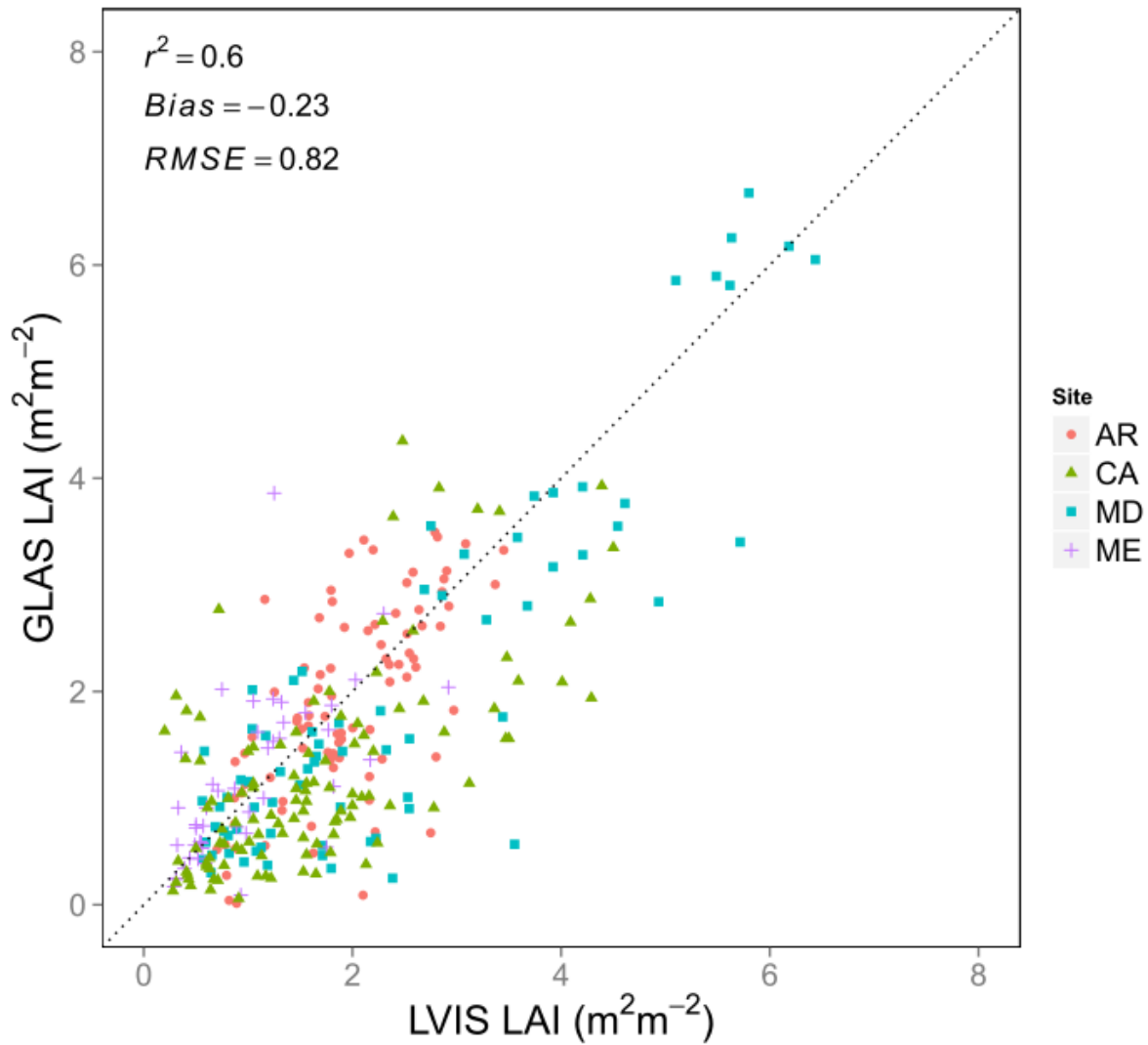
6

1 Table 1 Ecoregions with highest total LAI values (unit: $m^2 m^{-2}$)

Ecoregions	Total LAI Mean(\pm SD)	LAI 0-10m Mean(\pm SD)	LAI 10-20m Mean(\pm SD)	LAI >20m Mean(\pm SD)
Northern California coastal forests	5.24 \pm 2.11	2.06 \pm 1.32	1.67 \pm 1.09	1.08 \pm 1.15
Central Pacific coastal forests	5.00 \pm 2.14	1.52 \pm 1.61	1.10 \pm 1.16	0.84 \pm 1.25
British Columbia mainland coastal forests	4.74 \pm 2.26	1.48 \pm 1.31	1.23 \pm 1.08	1.13 \pm 1.13
Central and Southern Cascades forests	4.31 \pm 2.34	1.06 \pm 1.35	0.79 \pm 1.02	0.64 \pm 1.07
Klamath-Siskiyou forests	4.31 \pm 2.31	1.26 \pm 1.30	0.99 \pm 1.07	0.73 \pm 0.99
Willamette Valley forests	3.99 \pm 2.24	0.73 \pm 1.09	0.60 \pm 0.89	0.75 \pm 1.31
Appalachian-Blue Ridge forests	3.95 \pm 2.03	1.04 \pm 1.27	0.82 \pm 0.99	0.47 \pm 0.82
Puget lowland forests	3.91 \pm 2.25	0.98 \pm 1.39	0.71 \pm 1.08	0.40 \pm 0.81
Appalachian mixed mesophytic forests	3.86 \pm 2.04	1.06 \pm 1.29	0.77 \pm 0.93	0.48 \pm 0.83
North Central Rockies forests	3.67 \pm 2.27	1.61 \pm 1.55	0.84 \pm 0.89	0.47 \pm 0.72

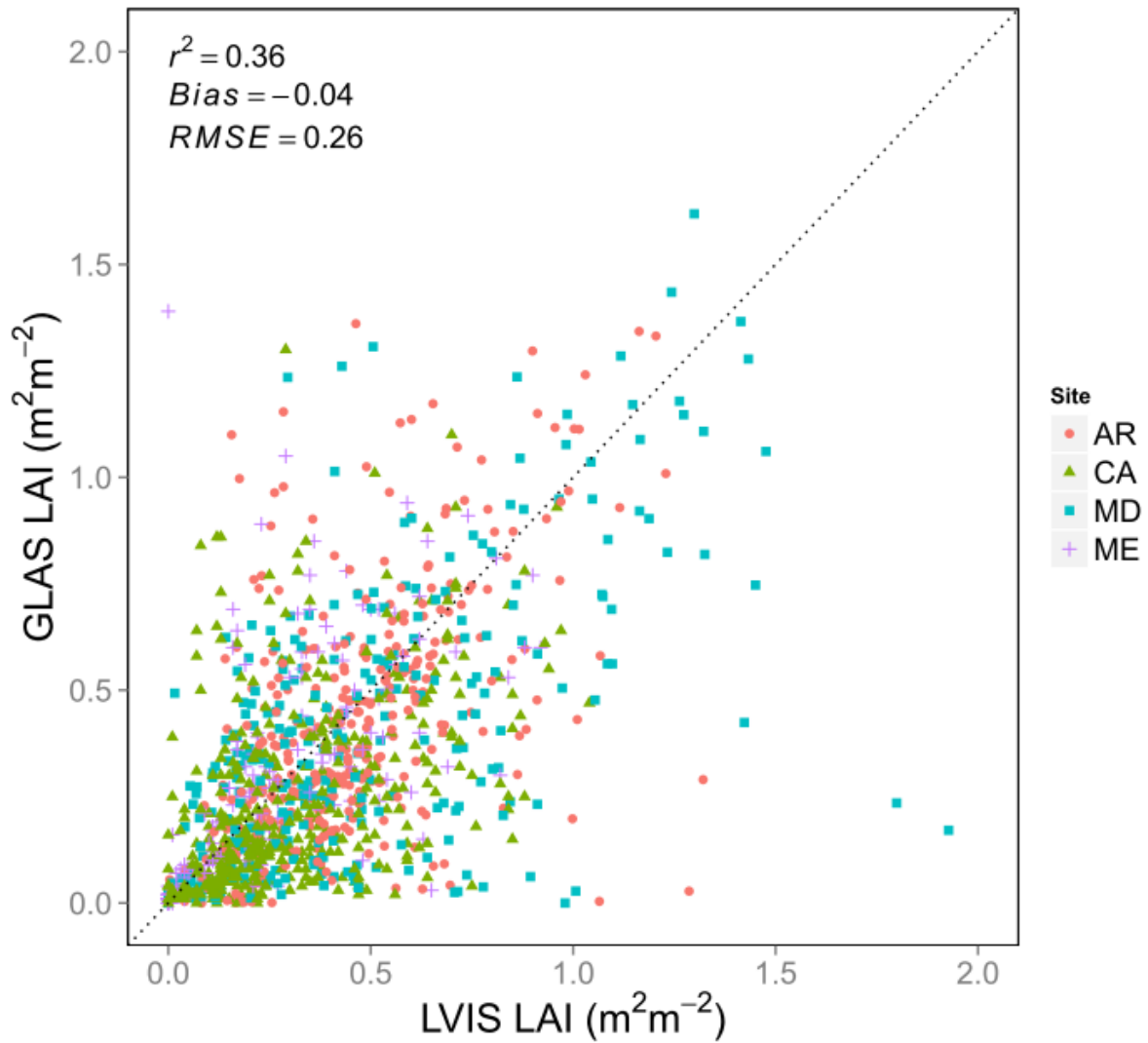
2

3



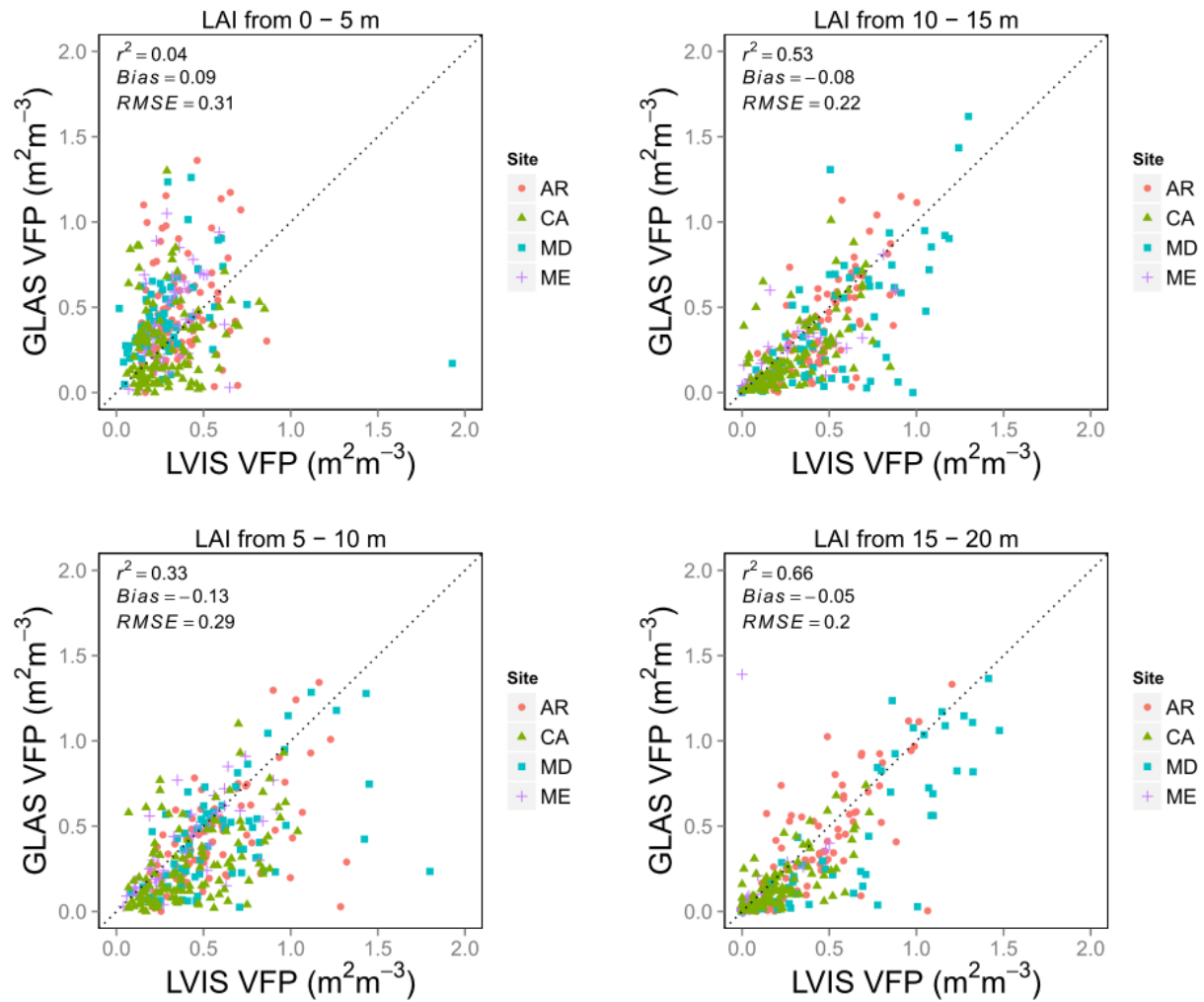
1

2 Fig. 1 A comparison between two lidar derived Leaf Area Index (LAI) datasets at different sites
 3 across the US (N = 318), produced from the Laser Vegetation Imaging Sensor (LVIS) and the
 4 Geoscience Laser Altimeter System (GLAS) respectively. Each point represents a comparison at
 5 GLAS footprint while different colors and shapes indicate different sites (AR: White River
 6 National Wildlife Refuge in Arkansas; CA: Sierra National Forest in California; MD:
 7 Baltimore/Washington corridor in Maryland; ME: Maine forests to the north of Orono, Maine).
 8 The comparison produces r^2 of 0.60, bias of -0.23, and RMSE of 0.82). Dashed line is the 1:1 line.
 9



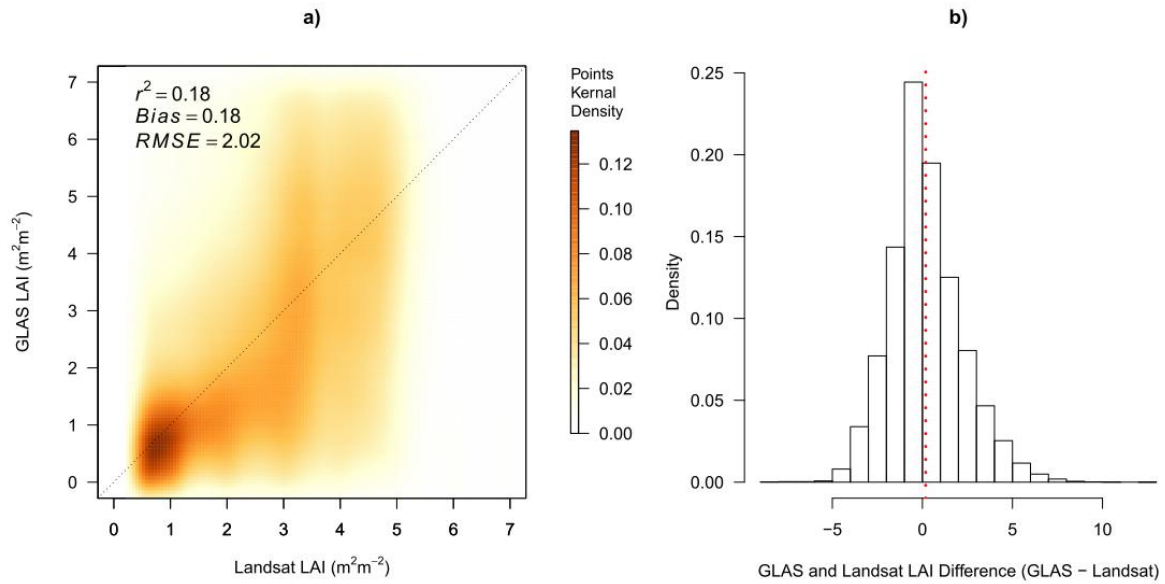
1

2 Fig. 2 A comparison of Vertical Foliage Profile (VFP) density derived from LVIS and GLAS
 3 over different sites in the US (same sites as Fig.1 but with N = 1272). Each VFP point represents
 4 an integrated value of foliage density at each 5 m height interval.



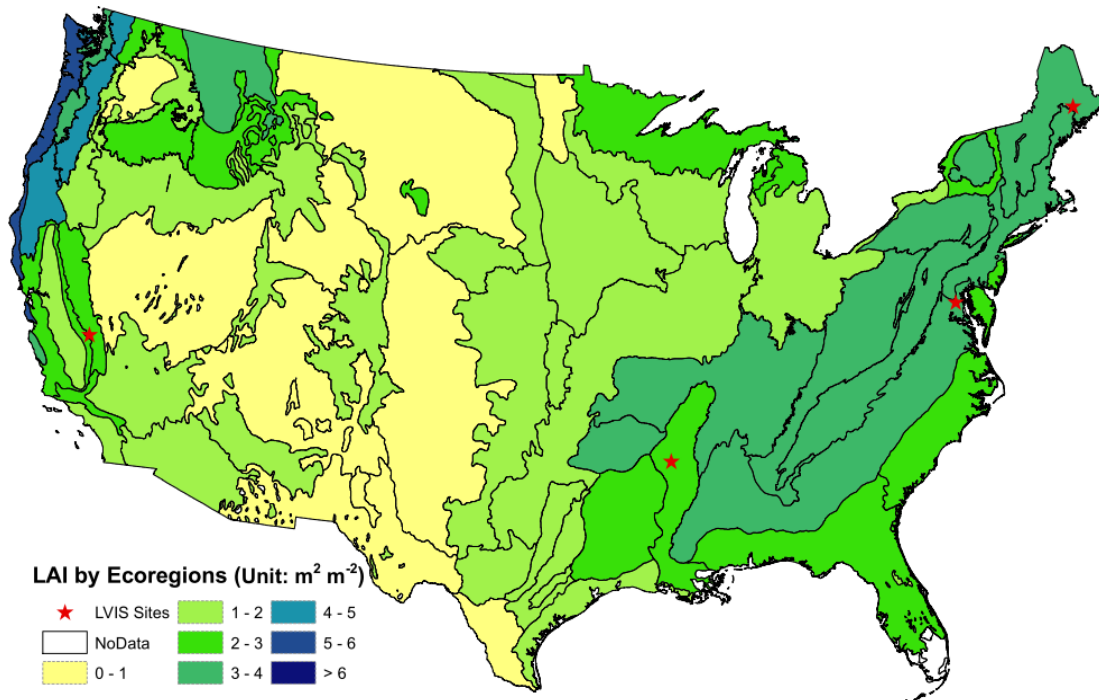
1
2

3 Fig. 3 Comparison between LVIS and GLAS VFP density integrated at every 5 m height interval
4 (from ground to canopy top).



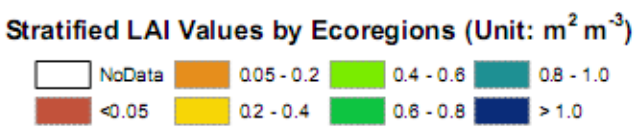
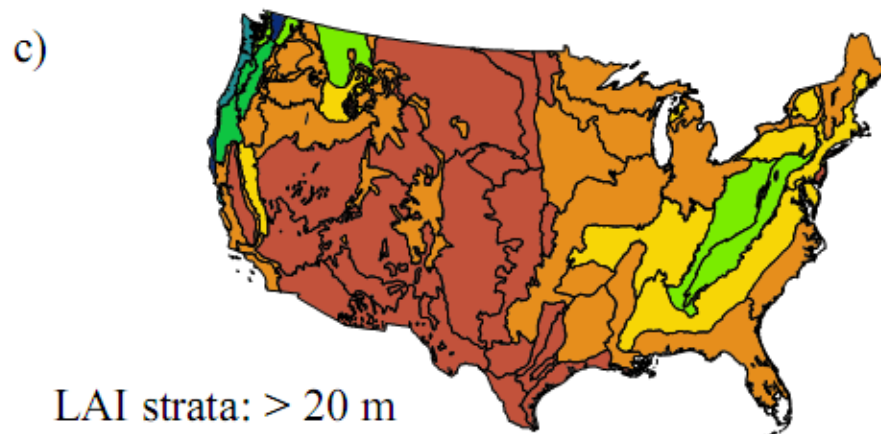
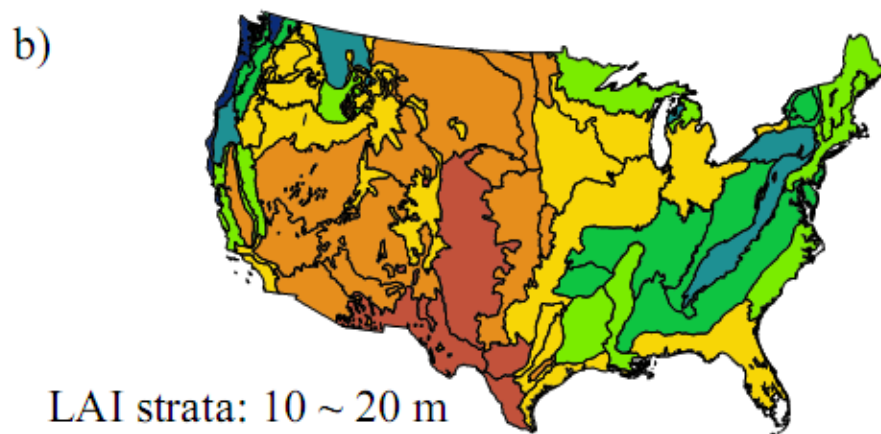
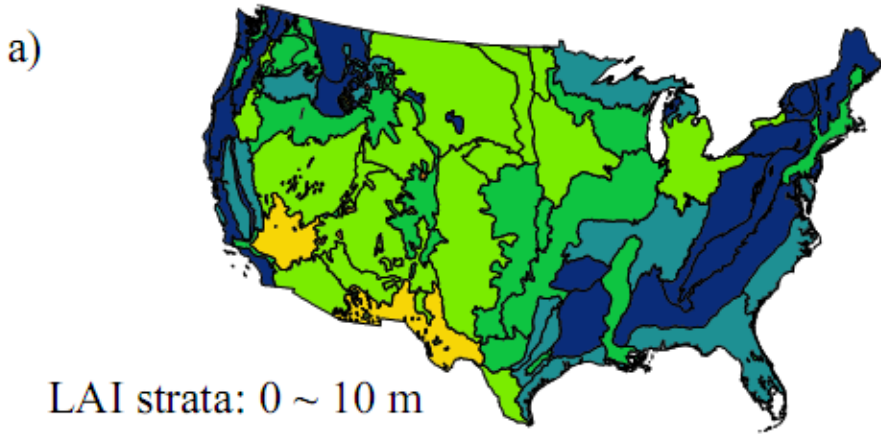
1
2

3 Fig. 4 Comparison between Landsat LAI and GLAS LAI over contiguous US: a) density scatter
 4 plot of Landsat and GLAS LAI ($r^2 = 0.18$, bias = 0.18 and RMSE = 2.02); b) Difference between
 5 Landsat and GLAS LAI. Darker kernel density color refers to more clustered distribution of LAI
 6 pairs.



1
2

3 Fig. 5 GLAS LAI distributions by ecoregion. All LVIS sites are marked with red stars.

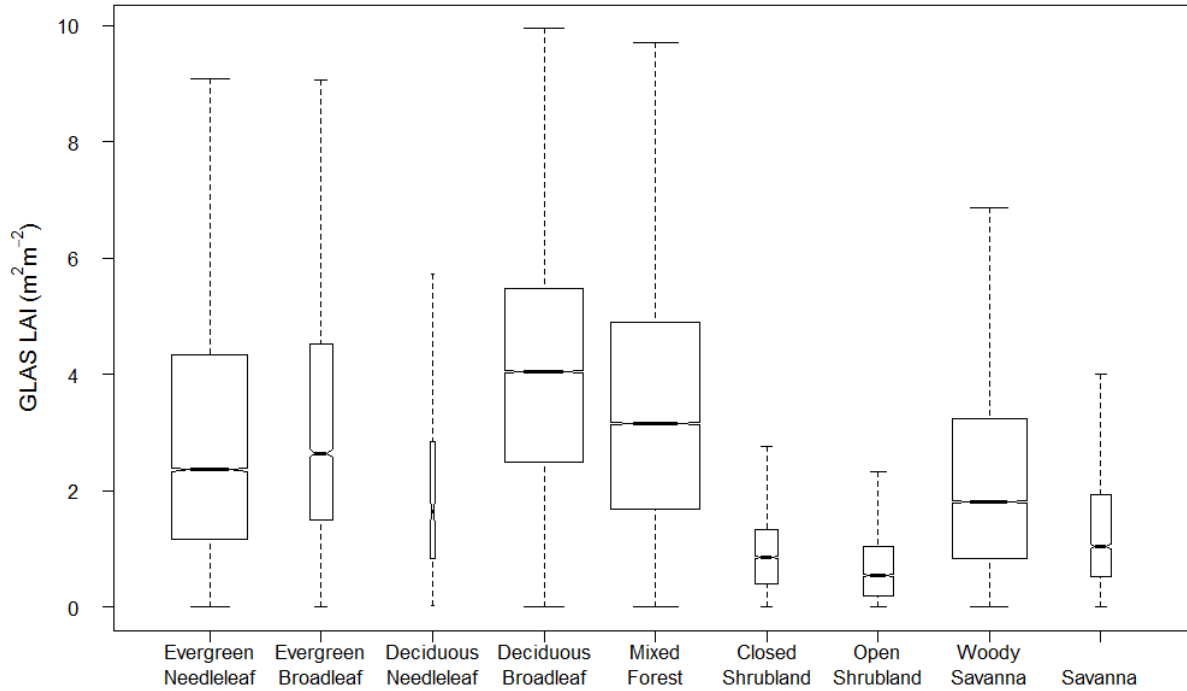


1

2

3

Fig. 6 LAI strata distributions by WWF ecoregions. Despite similar total LAI values, the southeastern forests show different LAI values at stratified height intervals.



1

2 Fig. 7 Distribution of total GLAS LAI across different land cover types. The width of the boxes is

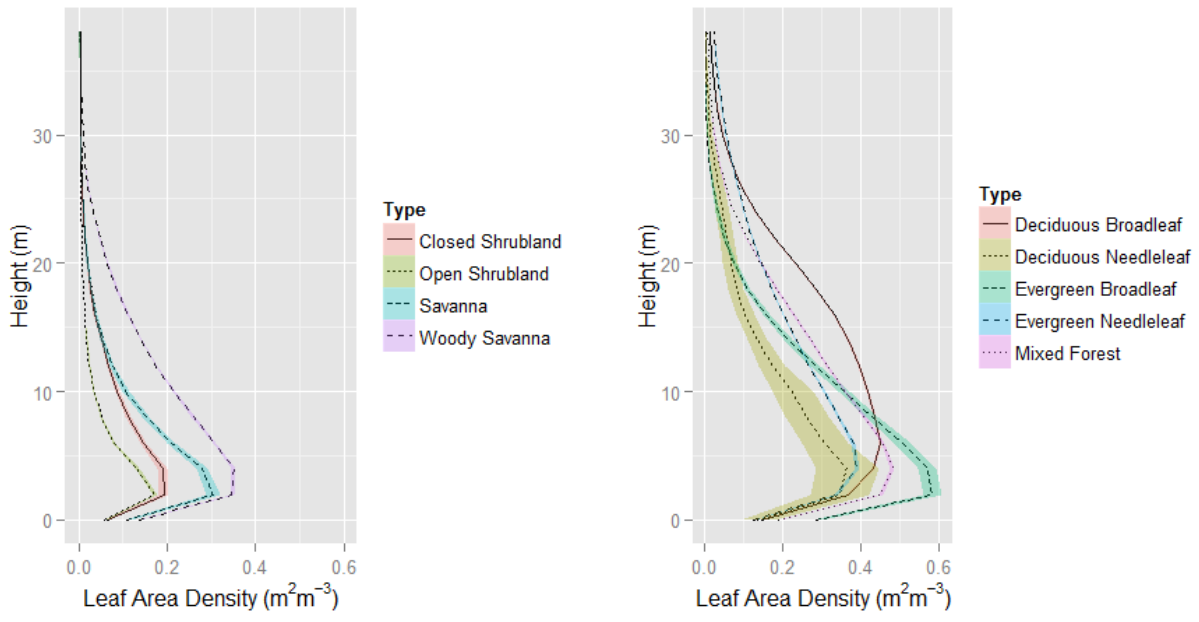
3 proportional to the number of observations for each type (N = Evergreen Needleleaf: 45207,

4 Evergreen Broadleaf: 438, Deciduous Needleleaf: 123, Deciduous Broadleaf: 48283, Mixed

5 Forest: 62053, Closed Shrubland: 4087, Open Shrubland: 7364, Woody Savanna: 43536,

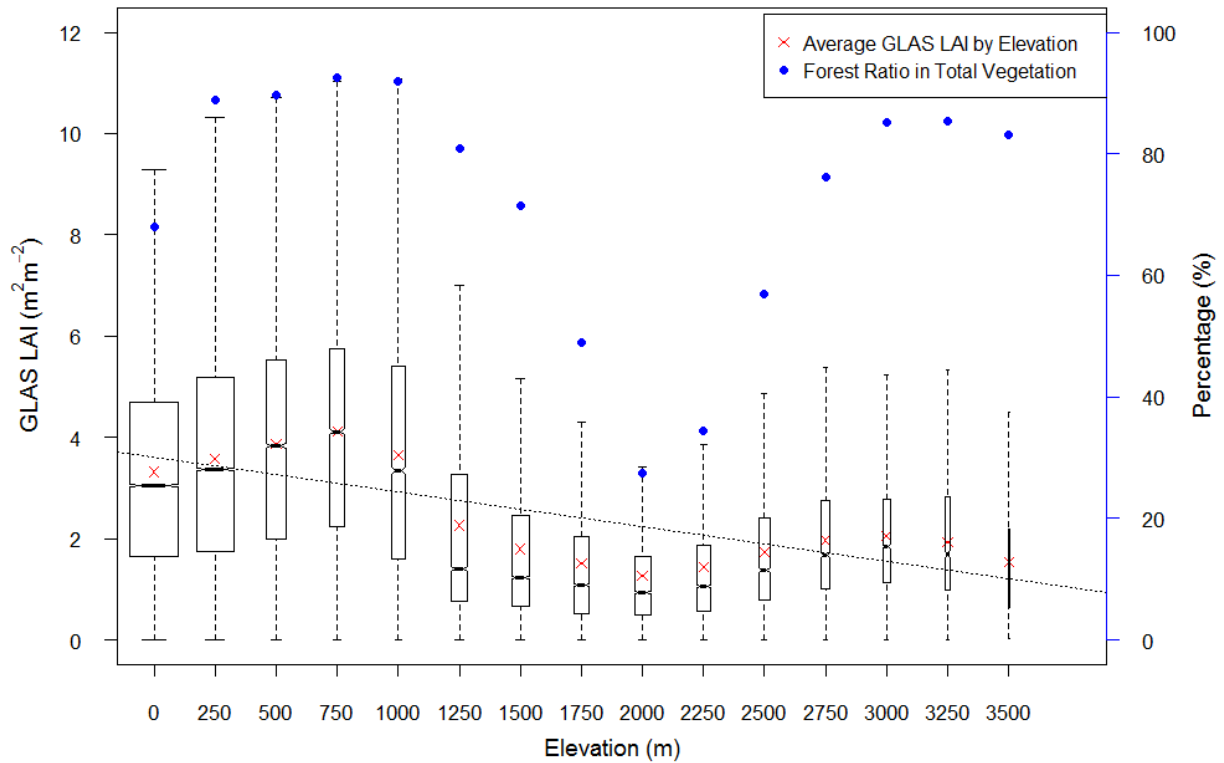
6 Savanna: 3051). Notches show the approximate 95% confidence interval of the median.

7



1

2 Fig. 8 Averaged GLAS VFP for different land cover types across US: non-forest vegetation types
 3 (left) and forest types (right). Mean values are central lines within the color-filled 95% CI
 4 envelope.



1

2 Fig. 9 Distribution of GLAS LAI (left axis) and Forest Ratio - GLAS shots over forest divided by

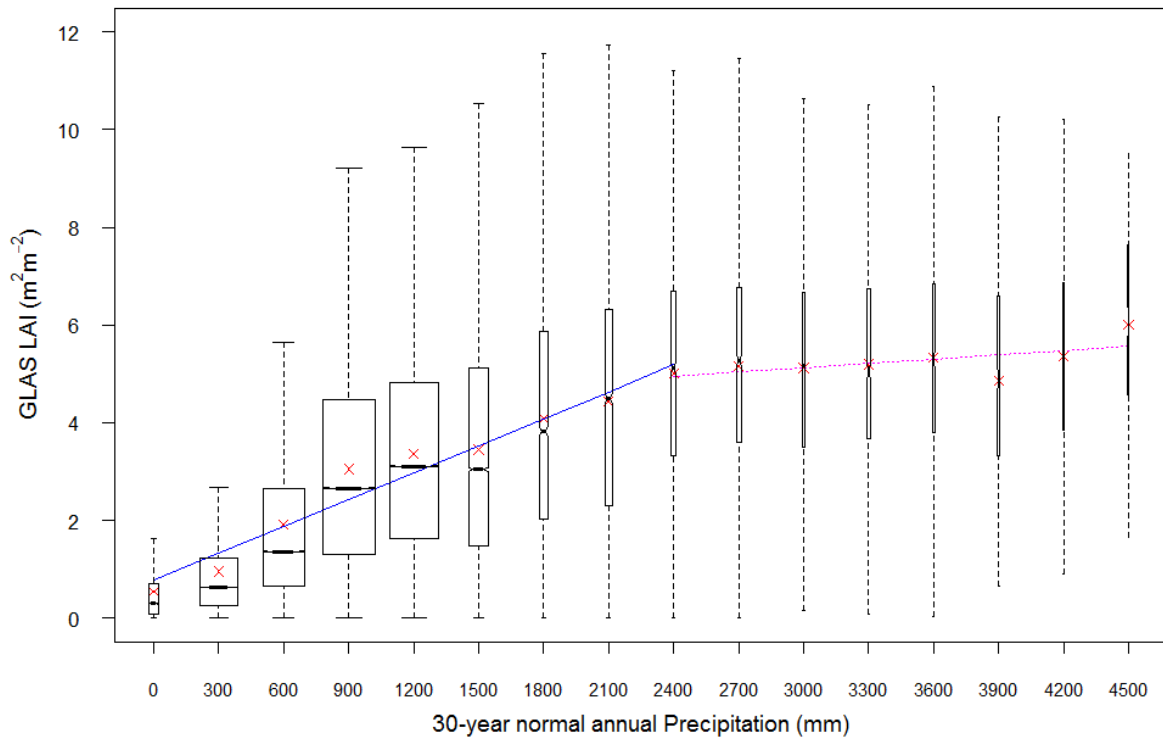
3 total shot numbers - (right axis). Overall, there is a decreasing trend of LAI values as elevation

4 increases, but deviations occur from this trend that are associated with elevational variation in

5 Forest Ratio—, which was defined as the percentage of footprints classified as forests in total GLAS

6 shots within each elevation group..

7



1
 2 Fig. 10 Distribution of GLAS LAI as a function of precipitation. A linear regression analysis of
 3 LAI values averaged by precipitation groups shows an increasing trend up to areas of about 2400
 4 mm (blue line). Beyond this value the rate of change slows considerably (magenta line) but the
 5 trend is only weakly significant ($P = 0.09$).

6
 7